Monitoring and Optimization for Power Grids

A signal processing perspective

Georgios B. Giannakis, Vassilis Kekatos, Nikolaos Gatsis,
Seung-Jun Kim, Hao Zhu, and Bruce F. Wollenberg

Although the North American power grid has been recognized as the most important engineering achievement of the 20th century, the modern power grid faces major challenges [87]. Increasingly complex interconnections even at the continent size render prevention of the rare yet catastrophic cascade failures a strenuous concern. Environmental incentives require carefully revisiting how electrical power is generated, transmitted, and consumed, with particular emphasis on the integration of renewable energy resources. Pervasive use of digital technology in grid operation demands resiliency against physical and cyberattacks on the power infrastructure. Enhancing grid efficiency without compromising stability and quality in the face of deregulation is imperative. Soliciting consumer participation and exploring new business opportunities facilitated by the intelligent grid infrastructure hold a great economic potential.

The smart grid vision aspires to address such challenges by capitalizing on state-of-the-art information technologies in sensing, control, communication, and machine learning [2], [24]. The resultant grid is envisioned to have an unprecedented level of situational awareness and controllability over its services and infrastructure to provide fast and accurate diagnosis/prognosis, operation resiliency upon contingencies and malicious attacks, as well as seamless integration of distributed energy resources.

BASIC ELEMENTS OF THE SMART GRID

A cornerstone of the smart grid is the advanced monitorability on its assets and operations. Increasingly pervasive installation of the phasor measurement units (PMUs) allows the so-termed synchrophasor measurements to be taken roughly 100 times faster than the legacy supervisory control and data acquisition (SCADA) measurements, time-stamped using the global positioning system (GPS) signals to capture the grid dynamics. In addition, the availability of low-latency, two-way communication

©COMSTOCK

networks will pave the way to high-precision, real-time grid state estimation and detection, remedial actions upon network instability, and accurate risk analysis and postevent assessment for failure prevention.

The provision of such enhanced monitoring and communication capabilities lays the foundation for various grid control and optimization components. Demand response (DR) aims to adapt the end-user power usage in response to energy pricing, which is advantageously controlled by utility companies via smart meters [29]. Renewable sources such as solar, wind, tidal, and electric vehicles (EVs) are important pieces of the future grid landscape. Microgrids will become widespread based on distributed energy sources that include distributed generation and storage systems. Bidirectional power flow to/from the grid due to such distributed sources has potentials to improve the grid economy and robustness. New services and businesses will be generated through open grid architectures and markets.

SIGNAL PROCESSING FOR THE GRID IN A NUTSHELL: PAST, PRESENT, AND FUTURE

Power engineers in the 1960s were facing the problem of computing voltages at critical points of the transmission grid, based on power flow readings taken at current and voltage transformers. Local personnel manually collected these readings and forwarded them by phone to a control center, where a set of equations dictated by Kirchoff's and Ohm's laws were solved for the electric circuit model of the grid. However, due to timing misalignment, instrumentation inaccuracy, and modeling uncertainties present in these measurements, the equations were always infeasible. Schweppe and others offered a statistical signal processing (SP) problem formulation and advocated a least-squares approach for solving it [69]—what enabled the power grid monitoring infrastructure used almost invariant until now [57], [1].

This is a simple but striking example of how SP expertise can have a strong impact in power grid operation. Moving from the early 1970s to today, the environment of the power system operation has become considerably more complex. New opportunities have emerged in the smart grid context, necessitating a fresh look. As will be surveyed in this article, modern grid challenges urge for innovative solutions that tap into diverse SP techniques from estimation, machine learning, and network science.

Avenues where significant contribution can be made include power system state estimation (PSSE) in various renditions, as well as "bad data" detection and removal. As costly large-scale blackouts can be caused by rather minor outages in distant parts of the network, wide-area monitoring of the grid turns out to be a challenging yet essential goal [78]. Opportunities abound in synchrophasor technology, ranging from judicious placement of PMUs to their role in enhancing observability, estimation accuracy, and bad data diagnosis. Unveiling topological changes given a limited set of power meter readings is a critical yet demanding task. Applications of machine learning to the power grid for clustering, topology inference, and big data

processing for, e.g., load/price forecasting constitute additional promising directions.

Power grid operations that can benefit from the SP expertise include also traditional operations such as economic dispatch, power flow, and unit commitment [84], [70], [25] as well as contemporary ones related to demand scheduling, control of plug-in EVs, and integration of renewables. Consideration of distributed coordination of the partaking entities along with the associated signaling practices and architectures require careful studies by the SP, control, and optimization experts.

Without any doubt, computationally intelligent approaches based on SP methodologies will play a crucial role in this exciting endeavor. From grid informatics to inference for monitoring and optimization tools, energy-related issues offer a fertile ground for SP growth for whose time has come.

MODELING PRELIMINARIES

Power systems can be thought of as electric circuits of even continent-wide dimensions. They obey multivariate versions of Kirchoff's and Ohm's laws, which in this section are overviewed using a matrix-vector notation. As the focus is laid on alternating current (ac) circuits, all electrical quantities involved (voltage, current, impedance, power) are complex valued. Further, quantities are measured in the per unit (p.u.) system, which means that they are assumed properly normalized. For example, if the "base voltage" is 138 kV, then a bus voltage of 140 kV is 1.01 p.u. The p.u. system enables uniform single- and three-phase system analysis, bounds the dynamic range of calculations, and allows for uniform treatment over the different voltage levels present in the power grid [84], [25].

Consider first a power system module of two nodes, m and n, connected through a line. A node, also referred to as a bus in the power engineering nomenclature, can represent, e.g., a generator or a load substation. A line (also known as *branch*) can stand for a transmission or distribution line (overhead/underground), or even a transformer. Two-node connections can be represented by the equivalent π model depicted in Figure 1 [99], [57], which entails the line series impedance $z_{mn} := 1/y_{mn}$ and the total charging susceptance $b_{c,mn}$. The former comprises a resistive part r_{mn} and a reactive (actually inductive) one $x_{mn} > 0$, that is $z_{mn} = r_{mn} + jx_{mn}$. The line series admittance $y_{mn} := 1/z_{mn} = g_{mn} + jb_{mn}$ is often used in place of the impedance. Its real and imaginary parts are called conductance and susceptance, respectively. Letting $\mathcal{V}_m$ denote the complex voltage at node m, $\mathcal{I}_{mn}$ the current flowing from node m to n, and invoking Ohm's and Kirchoff's laws on the circuit of Figure 1, yields

$$\mathcal{I}_{mn} = (jb_{c,mn}/2 + y_{mn})\,\mathcal{V}_m - y_{mn}\,\mathcal{V}_n. \qquad (1)$$

The reverse-direction current $\mathcal{I}_{nm}$ is expressed symmetrically. Unless $b_{c,mn}$ is zero, it holds that $\mathcal{I}_{nm} \neq -\mathcal{I}_{mn}$. A small shunt susceptance $b_{s,mm}$ is typically assumed between every node m and the ground (neutral), yielding the current $\mathcal{I}_{mm} = jb_{s,mm}\,\mathcal{V}_m$.

Building on the two-node module, consider next a power system consisting of a set $\mathcal{N}$ of N_b buses along with a set $\mathcal{E}$ of N_l transmission lines. By Kirchoff's current law, the complex

current at bus m denoted by $\mathcal{I}_m$ must equal the sum of currents on the lines incident to bus m; i.e.,

$$\mathcal{I}_m = \sum_{n \in \mathcal{N}_m} \mathcal{I}_{mn} + \mathcal{I}_{mm}$$
$$= \left(\sum_{n \in \mathcal{N}_m} y_{mn} + y_{mm} \right) \mathcal{V}_m - \sum_{n \in \mathcal{N}_m} y_{mn} \mathcal{V}_n, \quad (2)$$

where $\mathcal{N}_m$ is the set of buses directly connected to bus m, and $y_{mm} := j\left(b_{s,mm} + \sum_{n \in \mathcal{N}_m} b_{c,mn}/2 \right) := jb_{mm}$. Collecting node voltages (currents) in the $N_b \times 1$ vector $\mathbf{v}$ (i), leads to the multivariate Ohm's law

$$\mathbf{i} = \mathbf{Y}\mathbf{v}, \quad (3)$$

where $\mathbf{Y} \in \mathbb{C}^{N_b \times N_b}$ is the so-termed *bus admittance matrix* with (m, m)th diagonal entry $\sum_{n \in \mathcal{N}_m} y_{mn} + y_{mm}$ and (m, n)th off-diagonal entry $-y_{mn}$ if $n \in \mathcal{N}_m$, and zero otherwise [cf. (2)]. Matrix $\mathbf{Y}$ is symmetric and more importantly sparse, thus facilitating efficient storage and computations. On the contrary, the bus impedance matrix $\mathbf{Z}$, defined as the inverse of $\mathbf{Y}$ (and not as the matrix of bus pair impedances), is full and therefore it is seldom used.

A major implication of (3) is control of power flows. Let $\mathcal{S}_m := P_m + jQ_m$ be the complex power injected at bus m whose real and imaginary parts are the active (reactive) power P_m (Q_m). Physically, $\mathcal{S}_m$ represents the power generated and/or consumed by plants and loads residing at bus m. For bus m and with * denoting conjugation, it holds that $\mathcal{S}_m = \mathcal{V}_m \mathcal{I}_m^*$, or after collecting all power injections in $\mathbf{s} \in \mathbb{C}^{N_b}$ [diag($\mathbf{v}$) denotes a diagonal matrix holding $\mathbf{v}$ on its diagonal] one arrives at [cf. (3)]

$$\mathbf{s} = \mathrm{diag}(\mathbf{v})\mathbf{i}^* = \mathrm{diag}(\mathbf{v})\mathbf{Y}^*\mathbf{v}^*. \quad (4)$$

Complex power flowing from bus m to a neighboring bus n is similarly given by

$$\mathcal{S}_{mn} = \mathcal{V}_m \mathcal{I}_{mn}^*. \quad (5)$$

The ensuing analysis pertains mainly to nodal quantities. However, line quantities such as line currents and power flows over lines can be modeled accordingly using (1) and (5).

Typically, the complex bus admittance matrix is written in rectangular coordinates as $\mathbf{Y} = \mathbf{G} + j\mathbf{B}$. Two options become available from (4), depending on whether the complex nodal voltages are expressed in polar or rectangular forms. The polar representation $\mathcal{V}_m = V_m e^{j\theta_m}$ yields [cf. (2)]

$$P_m = \sum_{n=1}^{N_b} V_m V_n (G_{mn} \cos\theta_{mn} + B_{mn} \sin\theta_{mn}) \quad (6a)$$

$$Q_m = \sum_{n=1}^{N_b} V_m V_n (G_{mn} \sin\theta_{mn} - B_{mn} \cos\theta_{mn}), \quad (6b)$$

where $\theta_{mn} := \theta_m - \theta_n$ $\forall m$. Since P_m and Q_m depend on phase differences $\{\theta_{mn}\}$, power injections $\{\mathcal{S}_m\}$ are invariant to phase shifts of bus voltages. This explains why a selected bus called the
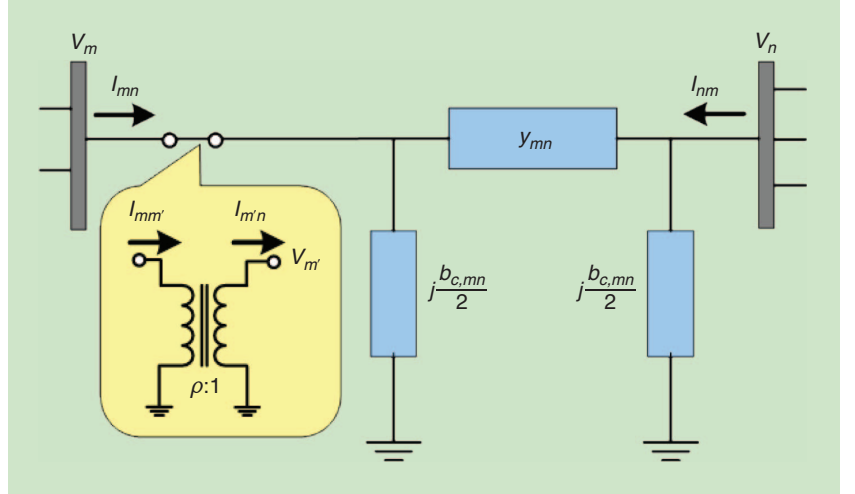
[FIG1] The equivalent π model for a transmission line; a yellow box when an ideal transformer is also present (cf. [10]).

reference, slack, or *swing* bus is conventionally assumed to have zero voltage phase without loss of generality.

If $\mathbf{Y}$ is known, the $2N_b$ equations in (6) involve the variables $\{P_m, Q_m, V_m, \theta_m\}_{m=1}^{N_b}$. Among the $4N_b$ nodal variables, 1) the reference bus has fixed (V_m, θ_m); 2) pairs (P_m, V_m) are controlled at generator buses (and are thus termed *PV buses*); while, 3) power demands (P_m, Q_m) are predicted for load buses (also called *PQ buses*). Fixing these $2N_b$ variables and solving the nonlinear equations (6) for the remaining ones constitutes the standard power flow problem [84, Ch. 4]. Algorithms for controlling PV buses and predicting load at PQ buses are presented in the sectrions "Economic Operation of Power Systems" and "Load and Electricity Price Forecasting," respectively.

Pairs (P_{mn}, V_{mn}) satisfying (approximately) power flow equations paralleling (6) can be found in [25, Ch. 3]. Among the approximations of the latter as well as (6), the so-called *direct current* (dc) *model* is reviewed next due to its importance in grid monitoring and optimization. The dc model hinges on three assumptions:

■ A1) The power network is purely inductive, which means that r_{mn} is negligible. In high-voltage transmission lines, the ratio $x_{mn}/r_{mn} = -b_{mn}/g_{mn}$ is large enough so that resistances can be ignored and the conductance part $\mathbf{G}$ of $\mathbf{Y}$ can be approximated by zero.

■ A2) In regular power system conditions, the voltage phase differences across directly connected buses are small; thus, $\theta_{mn} \simeq 0$ for every pair of neighboring buses (m, n), and the trigonometric functions in (6) are approximated as $\sin\theta_{mn} \simeq \theta_m - \theta_n$ and $\cos\theta_{mn} \simeq 1$.

■ A3) Due to typical operating conditions, the magnitude of nodal voltages is approximated by one p.u.

Under A1)–A3) and upon exploiting the structure of $\mathbf{B}$ [cf. (3)], the model in (6) boils down to

$$P_m = -\sum_{n \neq m} b_{mn} (\theta_m - \theta_n) \quad (7a)$$

$$Q_m = -b_{mm} - \sum_{n \neq m} b_{mn} (V_m - V_n), \quad (7b)$$

where $b_{mn} = -1/x_{mn}$ is the susceptance of the (m, n) branch, and in deriving (7), approximation of nodal voltage magnitudes to unity implies $V_m V_n \simeq 1$, yet $V_m(V_m - V_n) \simeq V_m - V_n$.

The dc model (7) entails linear equations that are neatly decoupled: active powers depend only on voltage phases, whereas reactive powers are solely expressible via voltage magnitudes. Furthermore, the linear dependence is on voltage differences. In fact, since $P_{mn} = -b_{mn}(\theta_m - \theta_n)$ and $b_{mn} < 0$, active power flows across lines from the larger- to the smaller-voltage phase buses.

Consider now the active subproblem described by (7a). Stacking the nodal real power injections in $\mathbf{p} \in \mathbb{R}^{N_b}$ and the nodal voltage phases in $\boldsymbol{\theta} \in \mathbb{R}^{N_b}$, leads to

$$\mathbf{p} = \mathbf{B}_x \boldsymbol{\theta}, \tag{8}$$

where the symmetric $\mathbf{B}_x$ is defined similar to $\mathbf{Y}$ by only accounting for reactances. Specifically, $[\mathbf{B}_x]_{mm} := \sum_{n \in \mathcal{N}_m} x_{mn}^{-1}$ for all m, and $[\mathbf{B}_x]_{mn} := -x_{mn}^{-1}$, if (m, n) line exists, and zero otherwise.

An alternative representation of $\mathbf{B}_x$ is presented next. Define matrix $\mathbf{D} := \mathrm{diag}(\{x_l^{-1}\}_{l \in \mathcal{E}})$, and the branch-bus $N_l \times N_b$ incidence matrix $\mathbf{A}$, such that if its lth row $\mathbf{a}_l^T$ corresponds to the (m, n) branch, then $[\mathbf{a}_l]_m := +1$, $[\mathbf{a}_l]_n := -1$, and zero elsewhere. Based on these definitions, $\mathbf{B}_x = \mathbf{A}^T \mathbf{D} \mathbf{A}$ can be viewed as a weighted Laplacian of the graph $(\mathcal{N}, \mathcal{E})$ describing the power network. This in turn implies that $\mathbf{B}_x$ is positive semidefinite, and the all-ones vector $\mathbf{1}$ lies in its null space. Further, its rank is $(N_b - 1)$ if and only if the power network is connected. Since $\mathbf{B}_x \mathbf{1} = \mathbf{0}$, it follows that $\mathbf{p}^T \mathbf{1} = 0$; stated differently, the total active power generated equals the active power consumed by all loads, since resistive elements and incurred thermal losses are ignored.

As a trivia, the terminology *dc model* stems from the fact that (8) models the ac power system as a purely resistive dc circuit by identifying the active powers, reactances, and the voltage phases of the former to the currents, resistances, and voltages of the latter.

Coming back to the exact power flow model of (4), consider now expressing nodal voltages in rectangular coordinates. If $\mathcal{V}_m = V_{r,m} + jV_{i,m}$ for all buses, it follows that

$$P_m = V_{r,m} \sum_{n=1}^{N_b} (V_{r,n} G_{mn} - V_{i,n} B_{mn})$$
$$+ V_{i,m} \sum_{n=1}^{N_b} (V_{i,n} G_{mn} + V_{r,n} B_{mn}) \tag{9a}$$
$$Q_m = V_{i,m} \sum_{n=1}^{N_b} (V_{r,n} G_{mn} - V_{i,n} B_{mn})$$
$$- V_{r,m} \sum_{n=1}^{N_b} (V_{i,n} G_{mn} + V_{r,n} B_{mn}). \tag{9b}$$

Based on (9a) and (9b), it is clear that (re)active power flows depend quadratically on the rectangular coordinates of nodal voltages. Because (9) is not amenable to approximations invoked in deriving (6), the polar representation has been traditionally preferred over the rectangular one.

Before closing this section, a few words are due on modeling transformers that were not explicitly accounted so far. Upon adding the circuit surrounded by the yellow square to the model of Figure 1, the possibility of having a transformer on a branch is considered in its most general setting [25], [99]. An ideal transformer residing on the (m, n) line at the mth bus side yields $\mathcal{V}_m = \mathcal{V}_{m'} \rho_{mn}$ and $\mathcal{I}_{m'n} = \rho_{mn}^* \mathcal{I}_{mm'}$, where $\rho_{mn} := \tau_{mn} e^{j\alpha_{mn}}$ is its turn ratio. Hence, (1) readily generalizes to

$$\begin{bmatrix} \mathcal{I}_{mn} \\ \mathcal{I}_{nm} \end{bmatrix} = \begin{bmatrix} \dfrac{y_{mn} + jb_{c,mn}/2}{|\rho_{mn}|^2} & -\dfrac{y_{mn}}{\rho_{mn}^*} \\ -\dfrac{y_{mn}}{\rho_{mn}} & y_{mn} + jb_{c,mn}/2 \end{bmatrix} \begin{bmatrix} \mathcal{V}_m \\ \mathcal{V}_n \end{bmatrix}. \tag{10}$$

Using (10) in lieu of (1), a similar analysis can be followed with the exception that in the presence of phase shifters, the corresponding bus admittance matrix $\mathbf{Y}$ will not be symmetric. Note though that the dc model of (8) holds as is, since it ignores the effects of transformers anyway.

The multivariate current-voltage law [cf. (3)], the power flow equations [cf. (6) or (9)], along with their linear approximation [cf. (8)] and generalization [(cf. (10)], will play instrumental roles in the grid monitoring, control, and optimization tasks outlined in the ensuing sections.

GRID MONITORING
In this section, SP tools and their roles in various grid monitoring tasks are highlighted, encompassing state estimation with associated observability and cyberattack issues, synchrophasor measurements, as well as intriguing inference and learning topics.

POWER SYSTEM STATE ESTIMATION
Simple inspection of the equations in the section "Grid Monitoring" confirms that all nodal and line quantities become available if one knows the grid parameters $\{y_{mn}\}$ and all nodal voltages $\mathcal{V}_{mn}$ that constitute the system state. Power system state estimation (PSSE) is an important module in the supervisory control and data acquisition (SCADA) system for power grid operation. Apart from situational awareness, PSSE is essential in additional tasks, particularly load forecasting, reliability analysis, the grid economic operations detailed in the section "Optimal Grid Operation," network planning, and billing [25, Ch. 4]. Building on the section "Modeling Preliminaries," this section reviews conventional solutions and recent advances, as well as pertinent smart grid challenges and opportunities for PSSE.

STATIC STATE ESTIMATION
Meters installed across the grid continuously measure electric quantities and forward them every few seconds via remote terminal units (RTUs) to the control center for grid monitoring. Due to imprecise time signaling and the SCADA scanning process, conventional metering cannot utilize phase information of the ac waveforms. Hence, legacy measurements involve (active/reactive) power injections and flows as well as voltage and current magnitudes on specific grid points. Given the SCADA measurements and assuming stationarity over a scanning cycle, the PSSE module estimates the state, particularly all complex nodal voltages collected in $\mathbf{v}$. Recall that according to the power flow models presented in the section "Modeling Preliminaries," all

grid quantities can be expressed in terms of $\mathbf{v}$. Thus, the $M \times 1$ vector of SCADA measurements can be modeled as $\mathbf{z} = \mathbf{h}(\mathbf{v}) + \boldsymbol{\epsilon}$, where $\mathbf{h}(\cdot)$ is a properly defined vector-valued function and $\boldsymbol{\epsilon}$ captures measurement noise and modeling uncertainties. Upon prewhitening, $\boldsymbol{\epsilon}$ can be assumed standard Gaussian. The maximum-likelihood estimate (MLE) of $\mathbf{v}$ can be then simply expressed as the nonlinear least-squares (LS) estimate

$$\hat{\mathbf{v}} := \arg\min_{\mathbf{v}} \| \mathbf{z} - \mathbf{h}(\mathbf{v}) \|_2^2. \tag{11}$$

Prior information, such as zero-injection buses ($P_m = Q_m = 0$) and feasible ranges (of V_m and θ_m), can be included as constraints in (11). In any case, the optimization problem is nonconvex. For example, when states are expressed in rectangular coordinates, the functions in $\mathbf{h}(\cdot)$ are quadratic; cf. (9). In general, PSSE falls under the class of nonlinear LS problems, for which Gauss–Newton iterations are known to offer the "workhorse" solution [1, Ch. 2]. Specifically, upon expressing $\mathbf{v}$ in polar coordinates, the quadratic $\mathbf{h}(\mathbf{v})$ can be linearized using Taylor's expansion around a starting point. The Gauss-Newton method hence approximates the cost in (11) with a linear LS one and relies on its minimizer to initialize the subsequent iteration. This iterative procedure is closely related to gradient descent algorithms for solving nonconvex problems, which are known to encounter two issues: 1) sensitivity to the initial guess and 2) convergence concerns. Without guaranteed convergence to the global optimum, existing variants improve numerical stability of the matrix inversions per iteration [1]. In a nutshell, the grand challenge so far remains to develop a solver attaining or approximating the global optimum at polynomial time.

Recently, a semidefinite relaxation (SDR) approach has been recognized to develop polynomial-time PSSE algorithms with the potential to find a globally optimal solution [95], [96]. Challenged by the nonconvexity of (11), the measurement model is reformulated as a linear function of the outer-product matrix $\mathbf{V} := \mathbf{v}\mathbf{v}^H$, where the state is now expressed in rectangular coordinates. This allows reformulating (11) to a semidefinite program (SDP) with the additional constraint $\text{rank}(\mathbf{V}) = 1$. Dropping the nonconvex rank constraint to acquire a convex SDP has been well appreciated in signal processing and communications; see, e.g., [52]. The SDR-based PSSE has been shown to approximate well the global optimum, while it is possible to further improve computational efficiency by exploiting the SDP problem structure [95].

DYNAMIC STATE ESTIMATION
As power systems evolve over time, dynamic PSSE is well motivated thanks to its predictive ability emerging when additional temporal information is available. In practice, it is challenged by both the unknown dynamics and the requirement of real-time implementation. While the latter could become tractable with (extended) Kalman filtering (KF) techniques, it is more difficult to develop simple state-space models to capture the power system dynamics.

There have been various proposals for state-transition models to perform the prediction step, mostly relying on a quasisteady state behavior; see [67] for a review of the main developments. One simplified and widely used model poses a "random-walk" behavior expressing the state in polar coordinates per time slot t as $\mathbf{v}(t + 1) = \mathbf{v}(t) + \mathbf{w}(t)$, where $\mathbf{w}(t)$ is zero-mean white Gaussian with a diagonal covariance matrix estimated online [57]. A more sophisticated dynamical model reads $\mathbf{v}(t + 1) = \mathbf{F}(t)\mathbf{v}(t) + \mathbf{e}(t) + \mathbf{w}(t)$, where $\mathbf{F}(t)$ is a diagonal transition matrix and $\mathbf{e}(t)$ captures the process mismatch. Recently, a quasi-static state model has been introduced to determine $\mathbf{e}(t)$ by approximating first-order effects of load data [7].

For the correction step, the extended KF (EKF) is commonly used via linearizing the measurement model around the state predictor [57], [67]. To overcome the reduced accuracy of EKF linearization, unscented KF (UKF) of higher complexity has been reported in [81]. Particle filtering may also be of interest if its computational efficiency can be tolerated by the real-time requirements of power systems.

DISTRIBUTED STATE ESTIMATION
Parallel and distributed solvers were investigated early on [69]. The motivation was primarily computational, even though additional merits of coordination across adjacent control areas were also recognized. In vertically integrated electricity markets, each local utility estimated its own state and modeled the rest of the system at boundary points using only local measurements. Adjacent power systems were connected via tie lines, which were basically used in emergency situations, and PSSE was performed locally with limited interaction among control centers.

Currently, the deregulation of energy markets has led to continent-wide interconnections that are split into subnetworks monitored by independent system operators (ISOs). An increasing amount of power is transferred over multiple control areas, and tie lines must be accurately monitored for reliability and accounting [27]. The ongoing penetration of renewables further intensifies long-distance power transfers, while their intermittent nature calls for frequent monitoring. Interconnection-level PSSE is therefore a key factor for modernizing power grids. Even though advanced instrumentation can provide precise and timely measurements (cf. the section "Phasor Measurement Units"), an interconnection could consist of thousands of buses. The latter together with privacy policies deem decentralized PSSE a pertinent solution.

To understand the specifications of distributed PSSE, consider the toy example of Figure 2. Area 2 consists of buses $\{3, 4, 7, 8\}$, but it also collects current measurements on tie lines $\{(4, 5), (4, 9), (7, 9)\}$. Its control center has two options regarding these measurements: either to ignore them and focus on the internal state, or to consider them and augment its state by the external buses $\{5, 9\}$. The first option is statistically suboptimal; let alone it may incur observability loss (check for example Area 3). For the second option, neighboring areas should consent on shared variables. This way, agreement is achieved over the line charges and the global PSSE problem is optimally solved.
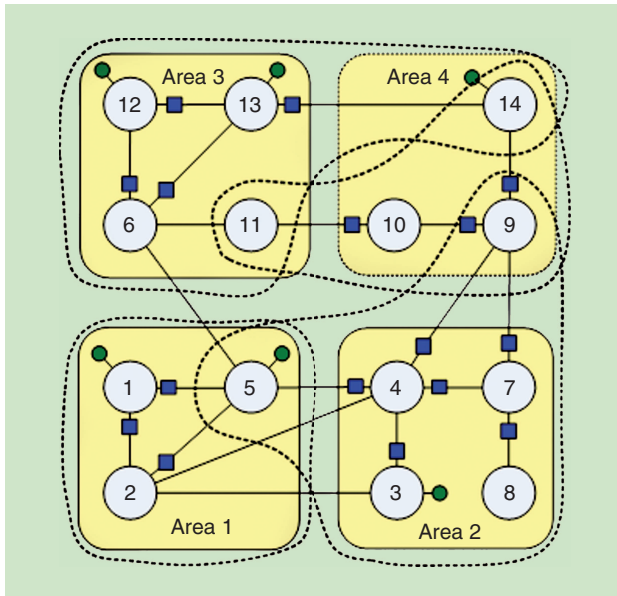
[FIG2] The IEEE 14-bus power system partitioned into four areas. Dotted lassos show the buses belonging to extended area states. PMU bus voltage (line current) measurements are depicted by green circles (blue squares).

It was realized early that, for a chain of serially interconnected areas, KF-type updates can be implemented incrementally in space [69, Pt. III]. For arbitrarily connected areas though, a two-level approach with a global coordinator is required [69]: local measurements involving only local states are processed to estimate the latter. Local estimates of shared states, their associated covariance matrices, and tie line measurements are forwarded to a global coordinator. The coordinator then updates the shared states and their statistics. Several recent renditions of this hierarchical approach are available under the assumption of local observability [27], [28]. A central coordinator becomes a single point of failure, while the sought algorithms may be infeasible due to computational, communication, or policy limitations. Decentralized solutions include block Jacobi iterations [16] and the auxiliary problem principle [19]. Local observability is waived in [88], where a copy of the entire high-dimensional state vector is maintained per area, and linear convergence of the proposed first-order algorithm scales unfavorably with the interconnection size. A systematic framework based on the alternating direction method of multipliers is put forth in [34]. Depending solely on existing PSSE software, it respects privacy policies, exhibits low communication load, and its convergence is guaranteed even in the absence of local observability. Finally, for a survey on multi-area PSSE, refer to [28].

GENERALIZED STATE ESTIMATION
PSSE presumes that grid connectivity and the electrical parameters involved (e.g., line admittances) are known. Since these are oftentimes unavailable, generalized state estimation (G-SE) extends the PSSE task to jointly recovering them too [1, Ch. 8], [25, Sec. 4.10]. PSSE operates on the bus/branch grid model; cf.

Figure 3(a). A more meticulous view of this grid is offered by the corresponding bus section/switch model depicted in Figure 3(b). This shows how a bus is partitioned by circuit breakers into sections (e.g., bus 1 to sections $\{1, 15 - 19\}$), or how a substation can appear as two different buses (e.g., sections $\{10, 52 - 54\}$ and $\{14, 55 - 57\}$ mapped to buses 10 and 14, respectively). Circuit breakers are zero-impedance switching components and are used for seasonal, maintenance, or emergency reconfiguration of substations. For some of them, the status and/or the power they carry may be reported to the control center. A topology processing unit collects this information and validates network connectivity prior to PSSE [57].

Even though topology malfunctions can be detected by large PSSE residual errors, they are not easily identifiable [1]. Hence, joint PSSE with topology processing under the G-SE task has been a well-appreciated solution [57]. G-SE essentially performs state estimation using the bus section/switch model. Due to the zero impedances though, breaker flows are appended to the system state. For regular transmission lines of unknown status or parameters, G-SE augments the system state by their flows likewise. In any case, to tackle the increased state dimensionality, breakers of known status are treated as constraints: open (closed) breakers correspond to zero flows (voltage drops). Practically, not all circuit breakers are monitored; and even for those monitored, the reported status may be erroneous [1]. Today, G-SE is challenged further: the penetration of renewables and DR programs will cause frequent substation reconfigurations. Yet, G-SE can be aided by advanced substation automation and contemporary intelligent electronic devices (IEDs).

Identifying substation configuration errors has been traditionally treated by extending robust PSSE methods (cf. the section "Robust State Estimation by Cleansing Bad Data") to the G-SE framework. Examples include the largest normalized residual test and the least-absolute value and the Huber's estimators [1, Ch. 8]. To reduce the dimensionality of G-SE, an equivalent smaller-size model has been developed in [26]. The method in [37] leverages advances in compressive sampling and instrumentation technology. Upon regularizing the G-SE cost by ℓ_2-norms of selected vectors, it promotes block sparsity on real and imaginary pairs of suspected breakers.

OBSERVABILITY, BAD DATA, AND CYBERATTACKS
The PSSE module presumes that meters are sufficiently many and well distributed across the grid so that the power system is observable. Since this may not always be the case, observability analysis is the prerequisite of PSSE. Even when the set of measurements guarantees system state observability, resilience to erroneous readings should be solicited by robust PSSE methods. Nonetheless, specific readings (un)intentionally corrupted can harm PSSE results. This section studies these intertwined topics.

OBSERVABILITY ANALYSIS
Given the network model and measurements, observability amounts to the ability of uniquely identifying the state v.

Even when the overall system is unobservable, power system operators are interested in observable islands. An observable island is a maximally connected subgrid, whose states become observable upon selecting one of its buses as a reference. Identifying observable islands is important because it determines which line flows and nodal injections can be uniquely recovered. Identifying unobservable islands further provides candidate locations for additional (pseudo)measurements needed to restore global observability. Pseudomeasurements are prior state information about, e.g., scheduled generations, forecasted loads, or predicted values (based on historical data) to aid PSSE in the form of measurements with high-variance additive noise (estimation error).

Due to instrument failures, communication delays, and network reconfigurations, observability must be checked online. The analysis typically resorts to the dc model (7), and hence, it can be performed separately per active and reactive subproblems thanks to the P-θ and Q-V decoupling. Since power measurements oftentimes come in (re)active pairs, the observability results obtained for the active subproblem described by (8) carry over to the reactive one, assuming additionally that at least one nodal voltage magnitude is available per observable island (the reactive analog of the reference bus).

Commonly used observability checks include topological as well as numerical ones; see [1, Ch. 4] for a review. Topological observability testing follows a graph-theoretic approach [14]. Given the graph of the grid and the available set of measurements, this test builds a maximal spanning tree. Its branches are either lines directly metered or lines incident to a metered bus, while every branch should correspond to a different measurement. If such a tree exists, the grid is deemed observable; otherwise, the so-derived maximal spanning forest defines the observable islands.

On the other hand, numerical observability considers the identifiability of the noiseless approximate dc model $\mathbf{z} = \mathbf{H}\boldsymbol{\theta}$ [58]. Linear system theory asserts that
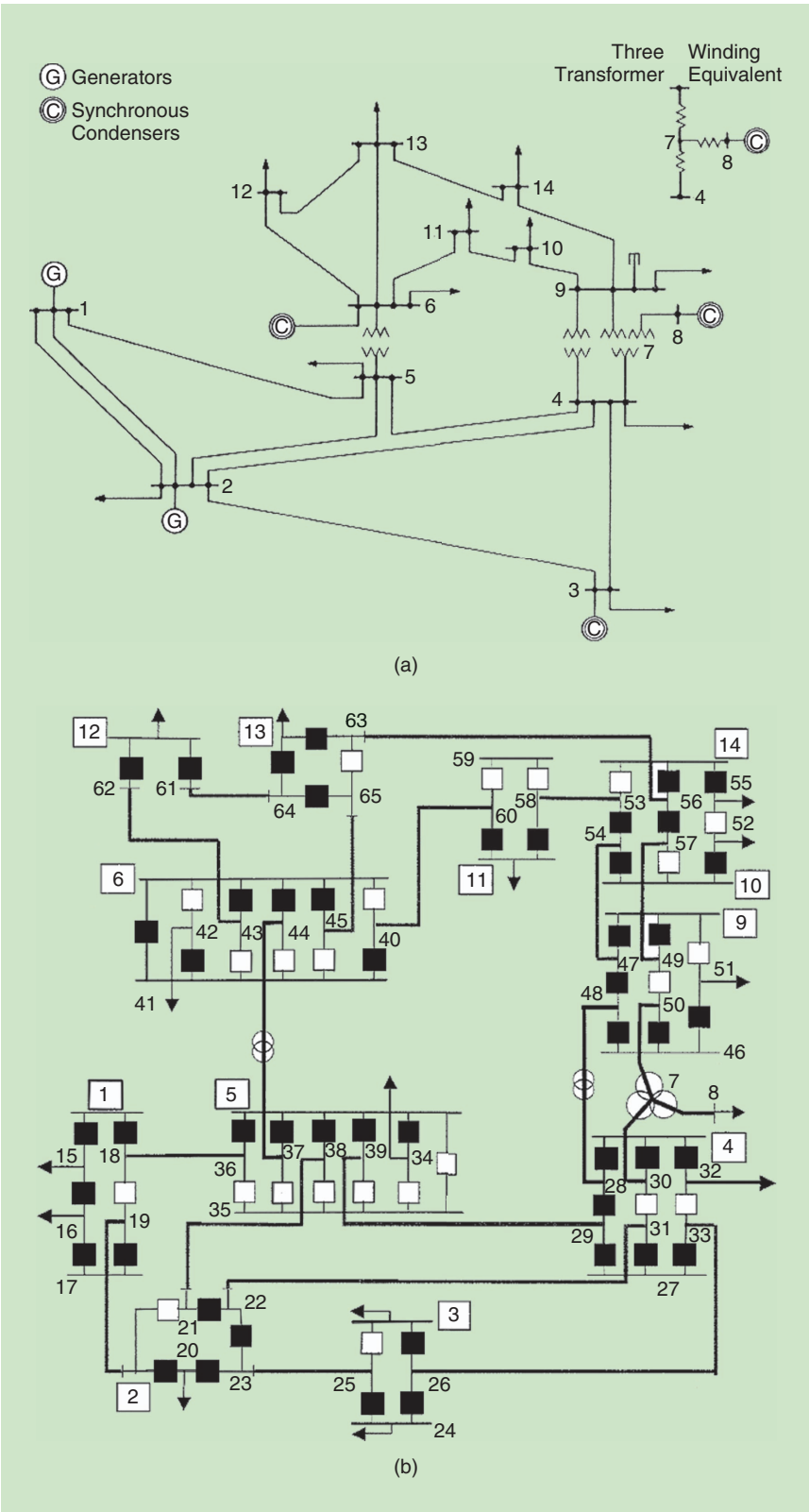
[FIG3] The IEEE 14-bus power system benchmark. (a) The conventional bus/branch model. (b) An assumed substation-level bus section/switch model [26]. Solid (hollow) squares indicate closed (open) circuit breakers. The original 14 buses preserve their numbering. Thick (thin) lines correspond to finite- (zero-) impedance transmission lines (circuit breaker connections). [Part (a) courtesy of [80]. Part (b) copyright *IEEE Transactions on Power Systems*.]

the state θ is observable if H is full column rank. Recall however that active power measurements introduce a voltage phase shift ambiguity [cf. (6) and (7)]. That is why a power system with branch-bus incidence matrix A is deemed observable simply if $A\theta = 0$ for every θ satisfying $H\theta = 0$, i.e., $\text{null}(H) \subseteq \text{null}(A)$. Observe now that the entries of $A\theta$ are proportional to line power flows. Hence, intuitively, whenever there is a nonzero power flow in the power grid, at least one of its measurements should be nonzero for it to be fully observable. When this condition does not hold, observable islands can be identified via the iterative process developed in [58].

ROBUST STATE ESTIMATION BY CLEANSING BAD DATA
Observability analysis treats all measurements received as reliable and trustworthy. Nonetheless, time skews, communication failures, parameter uncertainty, and infrequent instrument calibration can yield corrupted power system readings, also known as *bad data* in the power engineering parlance. If bad data pass through simple screening tests, e.g., polarity or range checks, they can severely deteriorate PSSE performance. Coping with them draws methods from robust statistical SP to identify outlying measurements, or at least detect their presence in the measurement set.

Two statistical tests, specifically the χ^2-test and the largest normalized residual test (LNRT), were proposed in [69, Part II] and are traditionally used for bad data detection and identification, respectively [57], [1, Ch. 5]. Both tests rely on the model $z = H\theta + \epsilon$, assuming a full column rank $m \times n$ matrix H and a zero voltage phase at the reference bus. The two tests check the residual error of the LS estimator that can be expressed as $r := Pz = P\epsilon$, where $P := I - H(H^T H)^{-1}H^T$ satisfying $P = P^T = P^2$. Apparently, when ϵ is standardized Gaussian, r is Gaussian too with covariance P; hence, $\|r\|_2^2$ follows a χ^2 distribution with $(m - n)$ degrees of freedom. The χ^2-test then declares an LS-based PSSE possibly affected by outliers whenever $\|r\|_2^2$ exceeds a predefined threshold.

The LNRT exploits further the Gaussianity of r. Indeed, as $r_i/\sqrt{P_{i,i}}$ should be standard Gaussian for all i when bad data are absent, the LNRT finds the maximum absolute value among these ratios and compares it against a threshold to identify a single bad datum [1, Sec. 5.7]. Practically, if a bad datum is detected, it is removed from the measurement set, and the LS estimator is recomputed. The process is repeated until no bad data are identified. Successive LS estimates can be efficiently computed using recursive least squares (RLS). The LNRT is essentially the leave-one-out approach, a classical technique for identifying single outliers. Interesting links between outlier identification and ℓ_0-pseudo norm minimization are presented in [42] and [34] under the Bayesian and the frequentist frameworks, respectively.

Apart from the two tests treating bad data a posteriori, outlier-robust estimators, such as the least-absolute deviation, the least median of squares, or Huber's estimator have been considered too; see [1]. Recently, ℓ_1-norm-based methods have been devised; see e.g., [42], [90], and [34].

Unfortunately, all bad data cleansing techniques are vulnerable to the so-called *critical measurements* [1]. A measurement is critical if, once removed from the measurement set, the power system becomes unobservable. If, for example, one removes the current measurement on line (7, 8) from the grid of Figure 2, then bus 8 voltage cannot be recovered. Actually, it can be shown that the ith measurement is critical if the ith column of P is zero, which translates to r_i being always zero too. Due to the latter, the LNRT is undefined for critical measurements.

Intuitively, a critical measurement is the only observation related to some state. Thus, this measurement cannot be cross-validated or questioned as an outlier, but it should be blindly trusted. The existence of critical measurements in PSSE reveals the connection between bad data and observability analysis. Apparently, the notion of critical measurements can be generalized to multiple simultaneously corrupted readings. Even though such events are naturally rare, their study becomes timely today under the threat of targeted cyberattacks as explained next.

CYBERATTACKS
As a complex cyberphysical system spanning a large geographical area, the power grid inevitably faces challenges in terms of cybersecurity. With more data acquisition and two-way communication required for the future grid, enhancing cybersecurity is of paramount importance. From working experience in dealing with the Internet and telecommunication networks, there is potential for malicious and well-motivated adversaries to either physically attack the grid infrastructure or remotely intrude the SCADA system. Among all targeted power grid monitoring and control operations, the PSSE task in the section "Power System State Estimation" appears to be of extreme interest as adversaries can readily mislead operators and manipulate electric markets by altering the system state [42], [89].

Most works analyzing cyberattacks consider the linear measurement model modified as $z = H\theta + \epsilon + a$, where the attack vector a has nonzero entries corresponding to compromised meters. It was initially pointed out in [50] that if the adversary knows H, the attack a can be constructed to lie in the range space of H so that the system operator can be arbitrarily misled. Under such a scenario, the attack cannot be detected. Such attacks are related to the observability and bad data analysis described earlier, since by deleting the rows of H corresponding to the nonzero entries of a, the resultant system becomes unobservable [42]. Various strategies to construct a have been derived in [50], constrained by the number of counterfeit meters; see also [42] for the minimum number of such meters. Cyberattacks under linear state-space models are considered in [63].

A major limitation of existing works lies in the linear measurement model assumption, not to mention the practicality of requiring attackers to know the full system configuration. Attacks in nonlinear measurement models for ac systems are studied in [97]. Granted that a nonlinear PSSE model can be approximated around a given state point, it is not obvious how

the attacker can acquire such dynamically varying information in real time to construct the approximation. This requires a per-adversary PSSE and assessment of a significant portion of meter measurements. On the defender's side, robustifying PSSE against bad data is a first countermeasure. Since cyberattacks can be judiciously designed by adversaries, they may be more challenging to identify, thus requiring further prior information, e.g., on the state vector statistics [42].

PHASOR MEASUREMENT UNITS

PHASOR ESTIMATION
PMUs are contemporary devices complementing legacy (SCADA) meters in advancing power system applications via their high-accuracy and time-synchronized measurements [65]. Different from SCADA meters that provide amplitude (power)-related information, PMUs offer also phase information. At the implementation level, current and voltage transformers residing at substations provide the analog input waveforms to a PMU. After antialias filtering, each one of these analog signals is sampled at a rate several times the nominal power system frequency f_0 (50–60 Hz). If the signal of interest has frequency f_0, its phasor information (magnitude and phase) can be obtained simply by correlating a window of its samples with the sampled cosine and sine functions, or equivalently by keeping the first (non-dc) discrete Fourier transform component. Such correlations can be implemented also recursively. Since power system components operate in the frequency range $f_0 \pm 0.5$ Hz, acquiring phasor information for off-nominal frequency signals has been also considered [65, Ch. 3].

The critical contribution of PMU technology to grid instrumentation is time-tagging. Using precise GPS timing (the 1 pulse/s signal), synchrophasors are time-stamped at the universal time coordinated (UTC). PMU data can thus be consistently aggregated across large geographic areas. Apart from phasors, PMUs acquire the signal frequency and its frequency derivative too. Data from several PMUs are collected by a phasor data concentrator (PDC), which performs time-aligning, local cleansing of bad data, and, potentially, data compression before forwarding data flows to the control center. IEEE standards C37.118.1/2-2011 determine PMU functional requirements.

PMU PLACEMENT
Although PMU technology is sufficiently mature, PMU penetration has been limited so far, mainly due to the installation and networking costs involved [78]. Being the key technology toward wide area monitoring though guarantees their wide deployment. During this instrumentation stage, prioritizing PMU locations is currently an important issue for utilities and reliability operators worldwide. Many PMU placement methods are based on the notion of topological observability; cf. the section "Observability Analysis." A search algorithm for placing a limited number of PMUs on a maximal spanning forest is developed in [61]. Even though topological observability in general does not imply numerical observability, for practical

measurement matrices it does [57]. In any case, a full column rank yet ill-conditioned linear regression matrix can yield numerically unstable estimators. Estimation accuracy rather than observability is probably a more meaningful criterion. Toward that end, PMU placement is formulated as a variation of the optimal experimental design problem in [48] and [35]. The approach in [48] considers estimating voltage phases only, ignores PMU current measurements, and proposes a greedy algorithm. In [35], the state is expressed in rectangular coordinates, all PMU measurements are considered, and the SDP relaxation of the problem is solved via a projected gradient algorithm. For a detailed review of PMU placements, the reader is referred to [53].

STATE ESTIMATION WITH PMUs
As explained in the section "Static State Estimation," PSSE is conventionally performed using SCADA measurements [84, Ch. 12]. PMU-based PSSE improves estimation accuracy when conventional and PMU measurements are jointly used [66], [65]. However, aggregating conventional and synchrophasor readings involves several issues. First, SCADA measurements are available every 4 s, whereas 30–60 synchrophasors can be reported per second. Second, explicitly including conventional measurements reduces the linear PMU-based PSSE problem into a nonlinear one. Third, compatibility to existing PSSE software and phase alignment should be also considered. An approach to address these challenges is treating SCADA-based estimates as pseudomeasurements during PMU-driven state estimation [65]. Essentially, the slower rate SCADA-based state estimates, expressed in rectangular coordinates, together with their associated covariance matrix can be used as a Gaussian prior for the faster rate linear PSSE problem based on PMU measurements [65], [35]. Regarding phase alignment, as already explained, SCADA-based estimates assume the phase of the reference bus to be zero, whereas PMUs record phases with respect to GPS timing. Aligning the phases of the two estimates can be accomplished by PMU-instrumenting the reference bus, and then simply adding its phase to all SCADA-based state estimates [65].

Synchrophasor measurements do not contribute only to PSSE. Several other monitoring, protection, and control tasks, ranging from local to interconnection-wide scope, can benefit from PMU technology. Voltage stability, line parameter estimation, dynamic line rating, oscillation and angular separation monitoring, and small signal analysis are just a few entries from the list of targeted applications [78], [65].

ADDITIONAL INFERENCE AND LEARNING ISSUES
PSSE offers a prototype class of problems to which SP tools can be readily employed to advance grid monitoring performance, especially after leveraging recent PMU technology to complement SCADA measurements. However, additional areas can benefit from SP algorithms applied to change detection, estimation, classification, prediction, and clustering aspects of the grid.
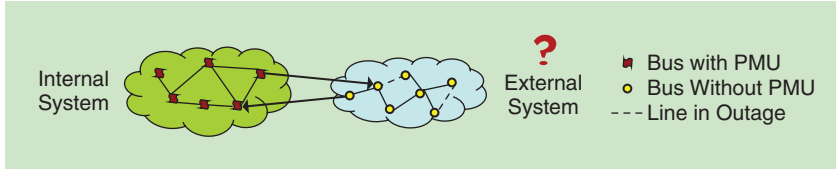
[FIG4] **The internal system to identify line outages occurring in the external system.**

LINE OUTAGE IDENTIFICATION

Unexpected events, such as a breaker failure, a tree falling, or a lightning strike, can make transmission lines inoperative. Unless the control center becomes aware of the outage promptly, power generation and consumption will remain almost unchanged across the grid. Due to flow conservation though, electric currents will be automatically altered in the outaged transmission network. Hence, shortly after, a few operating lines may exceed their ratings and successively fail. A cascading failure can spread over interconnected systems in a few minutes and eventually lead to a costly grid-wide blackout in less than an hour. Timely identifying line outages, or more generally abrupt changes in line parameters, is thus critical for wide-area monitoring.

One could resort to the generalized PSSE module to identify line outages (cf. the section "Generalized State Estimation"). Yet most existing topology processors rely on data of the local control area (also known as *internal*) system; see also Figure 4. On the other hand, flow conservation can potentially reveal line changes even in external systems. This would be a nonissue if intersystem data were available at a sufficiently high rate. Unfortunately, the system data exchange (SDX) module of the North American Electric Reliability Corporation (NERC) can provide the grid-wide basecase topology only on an hourly basis [76], while the desideratum here is near real-time line monitoring. In a nutshell, each internal system needs to timely identify line changes even in the external systems, relying only on local data and the infrequently updated basecase topology.

To concretely lay out the problem, consider the pre- and postevent states, and let $\tilde{\mathcal{E}} \subset \mathcal{E}$ denote the subset of lines in an outage. Suppose that the interconnected grid has reached a stable postevent state, and it remains connected [76]. With reference to the linear dc model in (8), its postevent counterpart reads $\mathbf{p}' = \mathbf{p} + \boldsymbol{\eta} = \mathbf{B}'_x \boldsymbol{\theta}'$, where $\boldsymbol{\eta}$ captures small zero-mean power injection perturbations. Recalling from the section "Modeling Preliminaries" that $\mathbf{B}_x = \mathbf{A}^T \mathbf{D} \mathbf{A}$, the difference $\tilde{\mathbf{B}}_x := \mathbf{B}_x - \mathbf{B}'_x$ can be expressed as $\tilde{\mathbf{B}}_x = \sum_{\ell \in \tilde{\mathcal{E}}} x_\ell^{-1} \mathbf{a}_\ell \mathbf{a}_\ell^T$. With $\boldsymbol{\theta}' := \boldsymbol{\theta}' - \boldsymbol{\theta}$, the "difference model" can be written as $\mathbf{B}\tilde{\boldsymbol{\theta}} = \sum_{\ell \in \tilde{\mathcal{E}}} m_\ell \mathbf{a}_\ell + \boldsymbol{\eta}$, where $m_\ell := \mathbf{a}_\ell^T \boldsymbol{\theta}'/x_\ell, \forall \ell \in \tilde{\mathcal{E}}$. Based on the latter, to identify $\tilde{\mathcal{E}}$ of a given cardinality $N_l^o := |\tilde{\mathcal{E}}|$, one can enumerate all $\binom{N_l}{N_l^o}$ possible topologies in outage, and select the one offering the minimum LS fit. Such an approach incurs combinatorial complexity, and has thus limited the existing exhaustive search methods to identifying single [76], or at most double, line outages [77]. A mixed-integer programming approach was proposed in [20], which again deals with single line outages.

To bypass this combinatorial complexity, [98] considers an overcomplete representation capturing all possible line outages. By constructing an $N_l \times 1$ vector $\mathbf{m}$, whose ℓth entry equals m_ℓ, if $\ell \in \tilde{\mathcal{E}}$, and 0 otherwise, it is possible to reduce the previous model to a sparse linear regression one given by

$$\mathbf{B}_x \tilde{\boldsymbol{\theta}} = \mathbf{A}^T \mathbf{m} + \boldsymbol{\eta}. \tag{12}$$

Since the control center only has estimates of the internal bus phases, it is necessary to solve (12) for $\tilde{\boldsymbol{\theta}}$ and extract the rows corresponding to the internal buses. This leads to a linear model slightly different from (12); but thanks to the overcomplete representation, identifying $\tilde{\mathcal{E}}$ amounts to recovering $\mathbf{m}$. The key point here is the small number of line outages ($N_{l,o} \ll N_l$) that makes the sought vector $\mathbf{m}$ sparse. Building on compressive sampling approaches, sparse signal recovery algorithms have been tested in [98] using IEEE benchmark systems, and near-optimal performance was obtained at computational complexity growing only linearly in the number of outages.

MODE ESTIMATION

Oscillations emerge in power systems when generators are interconnected for enhanced capacity and reliability. Generator rotor oscillations are due to lack of damping torque and give rise to oscillations of bus voltages, frequency, and (re)active power flows. Oscillations are characterized by the so-termed electromechanical modes, whose properties include frequency, damping, and shape [44]. Depending on the size of the power system, modal frequencies are often in the range of $0.1 - 2 \, \text{Hz}$. While a single generator usually leads to local oscillations at the higher range ($1 - 2 \, \text{Hz}$), interarea oscillations among groups of generators lie in the lower range ($0.1 - 1 \, \text{Hz}$). Typically, the latter ones are more troublesome, and without sufficient damping they grow in magnitude and may finally result in even grid breakups. Hence, estimating electromechanical modes, especially the low-frequency ones, is truly important and known as the small-signal stability problem in power system analysis [44].

Albeit near-and-dear to SP expertise on retrieving harmonics, modal estimation is challenging primarily due to the nonlinear and time varying properties of power systems, as well as the coexistence of several oscillation modes at nearby frequencies. Fortunately, the system behaves relatively linearly when operating at steady state and can thus be approximated by the continuous-time vector differential equations $\dot{\mathbf{x}}(t) = \mathbf{A}_x(t)\mathbf{x}(t) + \mathbf{B}_u \mathbf{u}(t) + \mathbf{w}(t)$, where the eigenvalues of $\mathbf{A}_x(t)$ characterize the oscillation modes, and $\mathbf{u}(t)$ and $\mathbf{w}(t)$ correspond to the exogenous input and the random perturbing noise, respectively. Assuming linear dynamic state models, mode estimation approaches are either model or measurement based. The former construct the exact nonlinear differential equations from system configurations and then linearize them at the steady-state to obtain $\mathbf{A}_x(t)$ for estimating

electromechanical modes [55]. In measurement-based methods, oscillation modes are acquired directly by peak-picking the spectral estimates obtained using linear measurements $\mathbf{x}(t)$ [79]. Since the complexity of model-based methods grows with the network size, scalability issues arise for larger systems. With PMUs, modes can be estimated directly from synchrophasors and even updated in real time.

Depending on the input $\mathbf{u}(t)$, the measurements are either ambient, ring-down (also known as *transient*), or probing; see, e.g., Figure 5. With only random noise $\mathbf{w}(t)$ attributed to load perturbations, the system operates under an equilibrium condition and the ambient measurements look like pseudonoise. A ring-down response occurs after some major disturbance, such as line tripping or a pulse input $\mathbf{u}(t)$, and results in observable oscillations. Probing measurements are obtained after intentionally injecting known pseudorandom inputs (probing signals) and can be considered as a special case of ring-down data. Missing entries and outliers are also expected in meter measurements, hence robust schemes are of interest for mode estimation [94]. Measurement-based algorithms can be either batch or recursive. In batch modal analysis, offline ring-down data are modeled as a sum of damped sinusoids and solved using, e.g., Prony's method to obtain linear transfer functions. Ambient data are handled by either parametric or nonparametric spectral analysis methods [79]. To recursively incorporate incoming data, several adaptive SP methods have been successfully applied, including least-mean squares (LMS) and RLS [94]. Apart from utilizing powerful statistical SP tools for mode estimation, it is also imperative to judiciously design efficient probing signals for improved accuracy with minimal impact to power system operations [79].

LOAD AND ELECTRICITY PRICE FORECASTING

The smooth operation of the grid depends heavily on load forecasts. Different applications require load predictions of varying time scales. Minute- and hour-ahead load estimates are fed to the unit commitment and economic dispatch modules as described in the section "Economic Operation of Power Systems." Predictions at the week scale are used for reliability purposes and hydrothermal coordination, while forecasts for years ahead facilitate strategic generation and transmission planning. The granularity of load forecasts varies spatially too, ranging from a substation, utility, to an interconnection level. Load forecasting tools are essential for electricity market participants and system operators. Even though such tools are widely used in vertically organized utilities, balancing supply and demand at a deregulated electricity market makes load forecasting even more important. At the same time, the introduction of EVs and DR programs further complicates the problem.

Load prediction can be simply stated as the problem of inferring future power demand given past observations. Oftentimes, historical and predicted values of weather data (e.g., temperature and humidity) are included as prediction variables too. The particular characteristics of power consumption render it an intriguing inference task. On top of a slowly increasing trend,
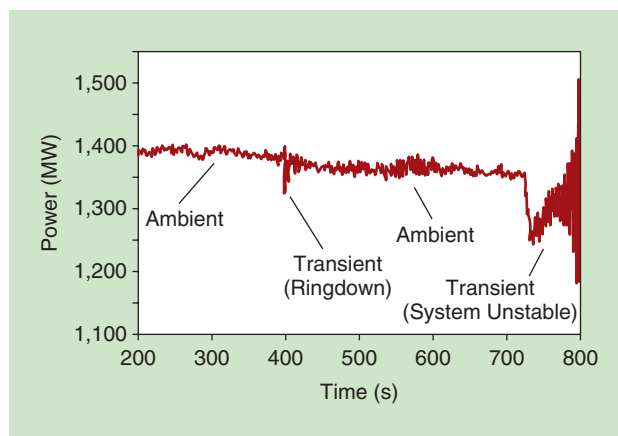
[FIG5] The real power flow on a major transmission line during the 1996 western North American power system breakup. (Figure used with permission from [79].)

load exhibits hourly, weekly, and seasonal periodicities. Holidays, extreme weather conditions, big events, or a factory interruption create outlying data. Moreover, residential, commercial, and industrial consumers exhibit different power profiles. Apart from the predicted load, uncertainty descriptors such as confidence intervals are important. Actually, for certain reliability and security applications, daily, weekly, or seasonal peak values are critically needed.

Several statistical inference methods have been applied for load forecasting: ordinary linear regression; kernel-based regression and support vector machines; time series analysis using autoregressive (integrated) moving average (with exogenous variables) models (ARMA, ARIMA, ARIMAX); state-space models with Kalman and particle filtering; and neural networks, expert systems, and artificial intelligence approaches. Recent academic works and current industry practices are variations and combinations of these themes reviewed in [70, Ch. 2]. Low-rank models for load imputation have been pursued in [54].

Load forecasting is not the only prediction task in modern power systems. Under a deregulated power industry, market participants can also leverage estimates of future electricity prices. To appreciate the value of such estimates, consider a day-ahead market: an ISO determines the prices of electric power scheduled for generation and consumption at the transmission level during the 24 hours of the following day. The ISO collects the hourly supply and demand bids submitted by generator owners and utilities. Using the optimization methods described later in the section "Economic Operation of Power Systems," the grid is dispatched in the most economical way while complying with network and reliability constraints. The output of this dispatch are the power schedules for generators and utilities, along with associated costs. Modern electricity markets are complex. Trading and hedging strategies, weather and life patterns, fuel prices, government policies, scheduled and random outages, and reliability rules—all these factors influence electricity prices. Even though prices are harder to predict than

loads, the task is truly critical in financial decision making [3]. The solutions proposed so far include econometric methods, physical system modeling, time series and statistical methods, artificial intelligence approaches, and kernel-based approaches; see, e.g., [3], [86], [36], and references therein.

GRID CLUSTERING

Modularizing power networks is instrumental for grid operation as it facilitates decentralized and parallel computation. Partitioning the grid into control regions can also be beneficial for implementing "self-healing" features, including islanding under contingencies [47]. For example, after catastrophic events, such as earthquakes, alternative power supplies from different management regions may be necessary due to power shortage and system instability. Furthermore, grid partitioning is essential for the zonal analysis of power systems, to aid load reliability assessment, and operational market analysis [8]. In general, it is imperative to partition the grid judiciously to cope with issues involving connected or disconnected "subgrids." The North American grid is currently partitioned in three interconnections, which are further divided into several zones for various planning and operation purposes. However, the static and manual grid partitioning currently in operation may soon become obsolete with the growing incorporation of renewables and the overall system scaling.

The clustering criterion must be in accordance with grid partitioning goals. In islanding applications, subgroups of generators are traditionally formed by minimizing the real generator-load imbalance to regulate the system frequency within each island. Recently, reactive power balance has been incorporated in a multiobjective grid partitioning problem to support voltage stability in islanding [47]. For these methods, it is necessary to reflect the real-time operating conditions that depend on the slow-coherency among generators, and the flow density along transmission lines.

Different from the islanding methods that deal with real-time contingencies, zonal analysis intends to address the long-term planning of transmission systems. Therefore, it is critical to define appropriate distance metrics between buses. Most existing works on long-term reliability have focused on the knowledge of network topology, including the seminal work of [83], which pointed out the "small-world" effects in power networks. To account for the structure imposed by Kirchhoff's laws, it was proposed in [8] to define "electrical distances" between buses using the inverse admittance matrix.

OPTIMAL GRID OPERATION

Leveraging the extensive monitoring and learning modalities outlined in the previous section, the next-generation grid will be operated with significantly improved efficiency and reduced margins. After reviewing classical results on optimal grid dispatch, this section outlines challenges and opportunities related to demand-response programs, electric vehicle charging, and the integration of renewable energy sources with particular emphasis on the common optimization tools engaged.

ECONOMIC OPERATION OF POWER SYSTEMS

ECONOMIC DISPATCH

Economic dispatch (ED) amounts to optimally setting the generation output in an electric power network so that the load is served and the cost of generation is minimized. ED pertains to generators that consume some sort of nonrenewable fuel to produce electric energy, the most typical fuel types being oil, coal, natural gas, or uranium. In what follows, a prototype ED problem is described, with focus placed on a specific time span, e.g., 10 min or 1 h, over which the generation output is supposed to be roughly constant.

Specifically, consider a network with N_g generators. Let P_{G_i} be the output of the ith generator in MWh. The cost of the ith generator is determined by a function $C_i(P_{G_i})$, which represents the cost in U.S. dollars for producing energy of P_{G_i} MWh (i.e., maintaining power output P_{G_i} MW for one hour). The cost $C_i(P_{G_i})$ is modeled as strictly increasing and convex, with typical choices including piecewise linear or smooth quadratic functions. The output of each generator is an optimization variable in ED, constrained within minimum and maximum bounds, $P_{G_i}^{\min}$ and $P_{G_i}^{\max}$, determined by the generator's physical characteristics [84, Ch. 2]. Since once a power plant is on, it has substantial power output, $P_{G_i}^{\min}$ is commonly around 25% of $P_{G_i}^{\max}$.

With P_L denoting the load forecasted as described in the section "Load and Electricity Price Forecasting," the prototype ED problem is to minimize the total generation cost so that there is supply-demand balance within the generators' physical limits

$$\min_{\{P_{G_i}\}} \quad \sum_{i=1}^{N_g} C_i(P_{G_i}) \tag{13a}$$

$$\text{subj. to} \quad \sum_{i=1}^{N_g} P_{G_i} = P_L \tag{13b}$$

$$P_{G_i}^{\min} \leq P_{G_i} \leq P_{G_i}^{\max}. \tag{13c}$$

Equation (13) is convex so long as the functions $C_i(P_{G_i})$ are convex. In this case, it can be solved very efficiently. Convex choices of $C_i(P_{G_i})$ offer a model approximating the true generation cost quite well and are used widely in the literature. Nevertheless, the true cost in practice may not be strictly increasing or convex, while the power output may be constrained to lie in a collection of disjoint subintervals $[P_{G_i}^{\min}, P_{G_i}^{\max}]$. These specifications make ED nonconvex and hence hard to solve. A gamut of approaches for solving the ED problem can be found in [84, Ch. 3].

Following a duality approach, suppose that Lagrange multiplier λ corresponds to the constraint in (13b). The multiplier has units \$/MWh, which has the meaning of price. Then, the KKT optimality condition implies that for the optimal generation output $P_{G_i}^*$ and the optimal multiplier λ^*, it holds that

$$P_{G_i}^* = \underset{P_{G_i}^{\min} \leq P_{G_i} \leq P_{G_i}^{\max}}{\operatorname{argmin}} \{C_i(P_{G_i}) - \lambda^* P_{G_i}\}, i = 1, \dots, N. \tag{14}$$

Due to (14), $C_i(P_{G_i}^*)$ is the ith generator's cost in dollars. Moreover, if λ^* is the price at which each generator is getting paid to

produce electricity, then $\lambda^* P_{G_i}^*$ is the profit for the ith generator. Hence, the minimum in (14) is the net cost, i.e., the cost minus the profit, for generator i. The latter reveals that the optimal generation dispatch is the one minimizing the net cost for each generator. If an electricity market is in place, ED is solved by the ISO, with $\{C_i(P_{G_i})\}$ representing the supply bids.

There are two take-home messages here. First, a very important operational feature of an electrical power network is to balance supply and demand in the most economical manner, and this can be cast as an optimization problem. Second, the Lagrange multiplier corresponding to the supply-demand balance equation can be readily interpreted as a price. However, the formulation in (13) entails two simplifying assumptions: 1) it does not account for the transmission network, and 2) it only pertains to a specific time interval, e.g., one hour. In practice, the power output across consecutive time intervals is limited by the generator physical characteristics. Even though the more complex formulations presented next alleviate these simplifications, the two take-home messages are still largely valid.

OPTIMAL POWER FLOW
The first generalization is to include the transmission network, using the dc load flow model of the section "Modeling Preliminaries"; cf. (8). The resultant formulation constitutes the dc optimal power flow (dc OPF) problem [12]. Specifically, it is postulated that at each bus there exists a generator and a load with output P_{G_m}, and demand P_{L_m}, respectively. The cases of no or multiple generators/loads on a bus can be readily accommodated.

Recall from (7a) that the real power flow from bus m to n is approximated by $P_{mn} \approx -b_{mn}(\theta_m - \theta_n)$. The bus angles $\{\theta_m\}$ are also variables in the dc OPF problem that reads

$$\min_{\{P_{G_m},\theta_m\}} \sum_{m=1}^{N_b} C_m(P_{G_m}) \tag{15a}$$

subj. to

$$P_{G_m} - P_{L_m} = -\sum_{n \in \mathcal{N}_m} b_{mn}(\theta_m - \theta_n), m = 1,\ldots,N_b \tag{15b}$$

$$P_{G_m}^{\min} \leq P_{G_m} \leq P_{G_m}^{\max}, m = 1,\ldots,N_b \tag{15c}$$

$$|P_{mn}| = |b_{mn}(\theta_m - \theta_n)| \leq P_{mn}^{\max}, m,n = 1,\ldots,N_b. \tag{15d}$$

The objective in (15a) is the total generation cost. The constraint in (15b) is the per bus balance. Specifically, the left-hand side of (15b) amounts to the net power injected to bus m from the generator and the load situated at the bus, while the right-hand side is the total power that flows toward all neighboring buses. Upon defining vectors for the generator and the load powers, (15b) could be written in vector form as $\mathbf{p}_G - \mathbf{p}_L = \mathbf{B}_x\boldsymbol{\theta}$ [cf. (8)]. Finally (15d) enforces power flow limits for line protection.

For convex generation costs $C_m(P_{G_m})$, the dc-OPF problem is convex too and, hence, efficiently solvable. A major consequence of considering per bus balance equations is that every

bus may have a different Lagrange multiplier. The pricing interpretation of Lagrange multipliers implies that a different price, called locational marginal price, corresponds to each bus. The ED problem in (13) can be thought of as a special case of dc OPF, where the entire network consists of a single bus on which all generators and loads reside.

Due to the dc load flow approximation, the accuracy of the dc OPF greatly depends on how well assumptions A1)–A3) hold for the actual power system. For better consistency with A2), it is further suggested to penalize the cost (15a) with the sum of squared voltage angle differences $\sum_{\text{lines}}(\theta_m - \theta_n)^2$, which retains convexity. Even if the dc OPF is a rather simplified model for actual power systems, it is worth stressing that it is used for the day-to-day operation in several North American ISOs.

Consider next replacing the dc with the ac load flow model (cf. the section "Modeling Preliminaries") in the OPF context. Generators and loads are now characterized not only by their real powers, but also the reactive ones, denoted as Q_{G_m} and Q_{L_m}. The ac OPF takes the form

$$\min_{\{P_{G_m},Q_{G_m},\mathbb{V}_m\}} \sum_{m=1}^{N_b} C_m(P_{G_m}) \tag{16a}$$

subj. to

$$P_{G_m} - P_{L_m} = \sum_{n \in \mathcal{N}_m} \text{Re}\{\mathcal{S}_{mn}\}$$

$$Q_{G_m} - Q_{L_m} = \sum_{n \in \mathcal{N}_m} \text{Im}\{\mathcal{S}_{mn}\} - b_{s,mm}|\mathcal{V}_m|^2 \tag{16b}$$

(5), (1)

$$P_{G_m}^{\min} \leq P_{G_m} \leq P_{G_m}^{\max}; Q_{G_m}^{\min} \leq Q_{G_m} \leq Q_{G_m}^{\max} \tag{16c}$$

$$|\text{Re}\{S_{mn}\}| \leq P_{mn}^{\max}; |S_{mn}| \leq S_{mn}^{\max}; V_m^{\min} \leq |\mathcal{V}_m| \leq V_m^{\max}. \tag{16d}$$

The constraint in (16b) reveals that now both the real and reactive powers must be balanced per bus. Recall further that $\mathcal{S}_{mn}$ represents the complex power flowing over line (m,n). Therefore, the first constraint in (16d) refers to the real power flowing over line (m,n) [cf. (15d)], while the second to the apparent power. The last constraint in (16d) calls for voltage amplitude limits.

Due to the nonlinear (quadratic equality) couplings between the power quantities and the complex voltage phasors, the ac OPF in (16) is highly nonconvex. Various nonlinear programming algorithms have been applied for solving it, including the gradient method, Newton–Raphson, linear programming, and interior-point algorithms; see, e.g., [84, Ch. 13]. These algorithms are based on the KKT necessary conditions for optimality and can only guarantee convergence to a stationary point at best. Taking advantage of the quadratic relations from voltage phasors to all power quantities as in SE, the SDR technique has been successfully applied, while a zero duality gap has been observed for many practical instances of the ac OPF and theoretically established for tree networks; see [46] and [45], and references therein. SDR-based solvers for three-phase OPF in distribution networks is considered in [17].

The ac OPF offers the most detailed and accurate model of the transmission network. Two main advantages over its dc counterpart are 1) the ability to capture ohmic losses and 2) its flexibility to incorporate voltage constraints. The former is possible because the resistive part of the line π-model is included in the formulation. Recall in contrast that assumption A1) in the dc model sets $r_{mn} = 0$. But it is exactly the resistive nature of the line that causes the losses. In view of (16), the total ohmic losses can be expressed as $\sum_m (P_{G_m} - P_{L_m})$. Such losses in the transmission network may be as high as 5% of the total load so that they cannot be neglected [25, Sec. 5.2].

The discussion on OPF—with dc or ac power flow—so far has focused on economic operation objectives. System reliability is another important consideration, and the OPF can be modified to incorporate security constraints too, leading to the security-constrained OPF (SCOPF). Security constraints aim to ensure that if a system component fails—e.g., if a line outage occurs—then the remaining system remains operational. Such failures are called contingencies. Specifically, the SCOPF aims to find an operating point such that even if a line outage occurs, all postcontingency system variables (powers, line flows, and bus voltages) are within limits. The primary concern is to avoid cascading failures that are the main reasons for system blackouts. As explained in the section "Line Outage Identification," if a line is in outage, the power flows on all other lines are adjusted automatically to carry the generated power.

SCOPF is a challenging problem due to the large number of possible contingencies. For the case of the dc OPF, power flows after a line outage are linearly related to the flows before the outage through the line outage distribution factors (LODFs) [12], [84, Ch. 11]. The LODFs can be efficiently calculated based on the bus admittance matrix $\mathbf{B}_x$ and are instrumental in the security-constrained dc OPF. The case of ac OPF is much more challenging, and a possible approach is enumeration of all possible contingency cases; see e.g., [84, Sec. 13.5] for different approaches.

UNIT COMMITMENT

Here, the scope of dc OPF is broadened to incorporate the scheduling of generators across multiple time periods, leading to the so-termed *unit commitment* (UC) problem. It is postulated that the scheduling horizon consists of periods labeled as $1, \ldots, T$ (e.g., a day consisting of 24 1-h periods). Let $P_{G_m}^t$ be the output of the mth generator at period t, and $P_{L_m}^t$ the respective demand. The generation cost is allowed to be time varying and is denoted by $C_m^t(P_{G_m}^t)$. A binary variable u_m^t per generator and period is introduced, so that $u_m^t = 1$ if generator m is on at t, and $u_m^t = 0$ otherwise. Moreover, the mth bus angle at t is denoted by θ_m^t.

Consideration of multiple time periods allows for inclusion of practical generator constraints into the scheduling problem. These are the ramp-up/down and minimum up/down time constraints. The former indicate that the difference in power generation between two successive periods is bounded. The latter mean that if a unit is turned on, it must stay on for a minimum number of hours; similarly, if it is turned off, it cannot be

turned back on before a number of periods. The UC problem is formulated as follows:

$$\min_{\{P_{G_m}^t, \theta_m^t, u_m^t\}} \sum_{t=1}^{T} \sum_{m=1}^{N_b} \left[C_m^t(P_{G_m}^t) + S_m^t(\{u_m^\tau\}_{\tau=0}^t) \right] \tag{17a}$$

subj. to

$$P_{G_m}^t = P_{L_m}^t - \sum_{n \in \mathcal{N}_m} b_{mn}(\theta_m^t - \theta_n^t), \; m = 1, \ldots, N_b, t = 1, \ldots, T \tag{17b}$$

$$u_m^t P_{G_m}^{\min} \le P_{G_m}^t \le u_m^t P_{G_m}^{\max}, m = 1, \ldots, N_b, t = 1, \ldots, T \tag{17c}$$

$$P_{G_m}^t - P_{G_m}^{t-1} \le R_m^{\text{up}}; P_{G_m}^{t-1} - P_{G_m}^t \le R_m^{\text{down}}, \\ m = 1, \ldots, N_b, t = 1, \ldots, T \tag{17d}$$

$$u_m^t - u_m^{t-1} \le u_m^\tau, \tau = t + 1, \ldots, \min\{t + T_m^{\text{up}} - 1, T\}, t = 2, \ldots, T \tag{17e}$$

$$u_m^{t-1} - u_m^t \le 1 - u_m^\tau, \\ \tau = t + 1, \ldots, \min\{t + T_m^{\text{down}} - 1, T\}, t = 2, \ldots, T \tag{17f}$$

$$|b_{mn}(\theta_m^t - \theta_n^t)| \le P_{mn}^{\max}, m, n = 1, \ldots, N_b, t = 1, \ldots, T \tag{17g}$$

$$u_m^t \in \{0, 1\}, m = 1, \ldots, N_b, t = 1, \ldots, T. \tag{17h}$$

The term $S_m^t(\{u_m^\tau\}_{\tau=0}^t)$ in the cost (17a) captures generator start-up or shut-down costs. Such costs are generally dependent on the previous on/off activity. For instance, the more time a generator has been off, the more expensive it may be to bring it on again. The initial condition u_m^0 is known. It is also assumed that $C_m^t(0) = 0$. The balance equation is given next by (17b). Generation limits are captured by (17c). The constraint in (17d) represents the ramp-up/down limits, where the bounds R_m^{up} and R_m^{down} and the initial condition $P_{G_m}^0$ are given. The constraint in (17e) means that if generator m is turned on at period t, it must remain on for the next T_m^{up} periods; and similarly for the minimum down time constraint in (17f), where both T_m^{up} and T_m^{down} are given [75]. The line flow constraints are given by (17g), while the binary feasible set for the scheduling variables u_m^t is shown in (17h).

It is clear that (17) is a mixed integer program. What makes it particularly hard to solve is the coupling across the binary variables expressed by (17e) and (17f). Note that the dc OPF in (15) is a special case of the UC (17) with the on/off scheduling fixed and the time horizon limited to a single period. It is noted in passing that a multiperiod version of the dc OPF can also be considered, by adding the ramp constraints to (15) while keeping the on/off scheduling fixed in (17), therefore obtaining a convex program. Most importantly, note that the UC dimension can be brought into the remaining two problems described here, i.e., the ED and the ac OPF. In the latter, the problem has two mathematical reasons for being hard, namely, the integer variables and the nonconvexity due to the ac load flow. The problems discussed here are illustrated in Figure 6.

A traditional approach to solving the UC is to apply Langrangian relaxation with respect to the balance equations [84, Ch. 5], [5], [75]. The dual problem can be solved by a nondifferentiable optimization method (e.g., a subgradient or bundle method), while the Lagrangian minimization step is solved via dynamic programming. An interesting result within the Lagrangian duality framework is that the duality gap of the UC problem

without a transmission network diminishes as the number of generators increases [5]. One of the state-of-the-art methods for UC is Benders' decomposition, which decomposes the problem into a master problem and tractable subproblems [70, Ch. 8].

DEMAND RESPONSE

~~DR~~ or load response is the adaptation of end-user power consumption to time-varying (or time-based) energy pricing, which is judiciously controlled by the utility companies to elicit desirable energy usage [24], [29]. The smart grid vision entails engaging residential end users in DR programs. Residential loads have the potential to offer considerable gains in terms of flexible load response, because their consumption can be adjusted—e.g., an air conditioning unit (A/C)—or deferred for later or shifted to an earlier time. Examples of flexible loads include pool pumps or plug-in (hybrid) EVs (PHEVs). The advent of smart grid technologies have also made available at the residential level energy storage devices (batteries), which can be charged and discharged according to residential needs, and thus constitute an additional device for control.

Widespread adoption of DR programs can bring significant benefits to the future grid. First, the peak demand is reduced as a result of the load shifting capability, which can have major economical benefits. Without DR, the peak demand must be satisfied by generation units such as gas turbines that can turn on and be brought in very fast during those peaks. Such units are very costly to operate and markedly increase the electricity wholesale prices. This can be explained in a simple manner by recalling the ED problem and specifically (14). Considering a gas turbine that is brought in and does not operate at its limits, (14) implies that $\lambda^* = C'(P^*_{G_{\text{turbine}}})$. Expensive units have exactly very high derivative C', i.e., increasing their power output requires a lot of fuel.

A second benefit of DR is that it has the potential to reduce the end-user bills. This is due to the time-based pricing schemes, which encourage consumption during reduced-price hours, but also because the wholesale prices become less volatile as explained earlier, which means that the electricity retailers can procure cheaper sources. A third benefit is that DR can strengthen the adoption of renewable energy. The reason is that the random and intermittent nature of renewable energy can be compensated by the ability of the load to follow such effects. More light into the latter concept will be shed in the section "Renewables."

DR is facilitated by deployment of the advanced metering infrastructure (AMI), which comprises a two-way communication network between utility companies and end users (see Figure 7) [24], [29]. Smart meters installed at end users' premises are the AMI terminals at the end users' side. These measure not just the total power consumption
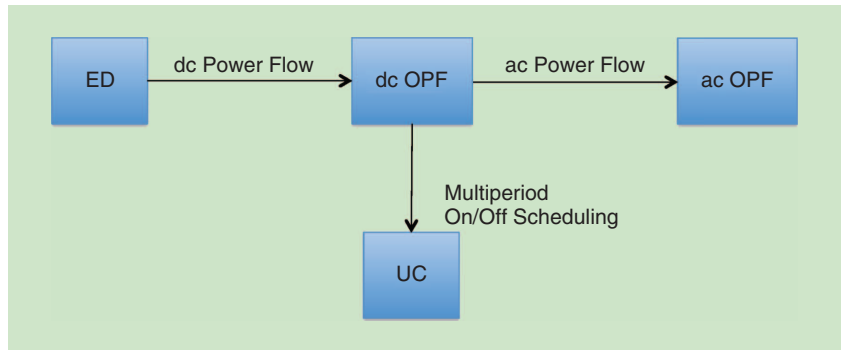

[FIG6] Relationship between the ED, OPF (dc and ac), and UC. From left to right: increasing detail in the transmission network model. From top to bottom: single- to multiperiod scheduling (also applicable to ED and ac OPF).

but also the power consumption profile throughout the day and report it to the utility company at regular time intervals—e.g., every 10 min or every 1 h. The utility company sends pricing signals to the smart meters through the AMI, for the smart meters to adjust the power consumption profile of the various residential electric devices, to minimize the electricity bill and maximize the end-user satisfaction. Energy consumption is thus scheduled through the smart meter. The communication network at the customer's premises between the smart meter and the smart appliances' controllers is part of the so-called home area network (HAN).

Time-varying pricing has been a classical research topic [10]. The innovation DR brings is that the end users' power consumption becomes controllable and, therefore, part of the system optimization. Novel formulations addressing the various research issues are therefore called for. DR-related research issues can be classified in two groups. The first group deals with joint optimization of DR for a set of end users, which will be termed hereafter *multiuser DR*. The second group focuses on optimal algorithm design for a single smart meter with the aim of minimizing the electricity bill and the user discomfort in response to real-time pricing signals. Each approach has unique characteristics, as explained next.

Multiuser DR sets a system-wide performance objective accounting for the cost of the energy provider and the user satisfaction. Joint scheduling must be performed in a distributed fashion, and much of the effort is to come up with pricing schemes that achieve this goal. The privacy of the customers must be protected, in the sense that they do not reveal their individual power consumption preferences to the utility, but the desired power consumption profile is elicited by the pricing
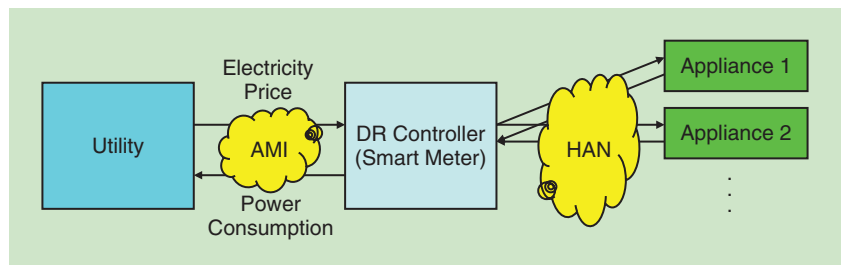
[FIG7] Communications infrastructure facilitating DR capabilities.

signals. One of the chief advantages of joint DR scheduling for multiple users is that the peak power consumption is reduced as compared to a baseline non-DR approach. The reason is that joint scheduling opens up the possibility of loads being arranged across time so that valleys are filled and peaks are shaved.

On the other hand, energy-consumption scheduling formulations for a single user can model in great detail the various smart appliance characteristics, often leading to difficult nonconvex optimization problems. This is in contrast with the vast majority of multiuser algorithms, which tend to adopt a more abstract and less refined description of the end users' scheduling capabilities. More details on the two groups of problems are given next.

MULTIUSER DR

Consider R residential end users, connected to a single load-serving entity (LSE), as illustrated in Figure 8. The LSE can be an electricity retailer or an aggregator, whose role is to coordinate the R users' consumption and present it as a larger flexible load to the main grid. The time horizon consists of T periods, which can be a bunch of 1-hr or 10-min intervals. User r has a set of smart appliances $\mathcal{A}_r$. Let p_{ra}^t be the power consumption of appliance a of user r at time period t (typically in kilowatthour), and $\mathbf{p}_{ra}$ a $T \times 1$ vector collecting the corresponding power consumptions across slots.

The LSE incurs cost $C^t(s^t)$ for providing energy s^t to the users. This cost is essentially the cost of energy procurement from the wholesale market or through direct contracts with energy generation units, and may also include other operation and maintenance costs. Each user also adopts a utility function $U_{ra}(\mathbf{p}_{ra})$, which represents user willingness to consume power.

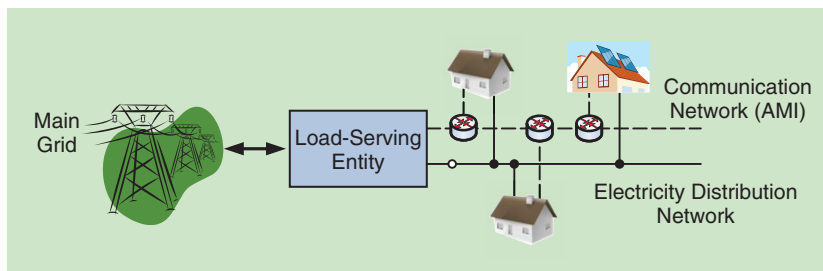The prototype multiuser DR problem takes the following form:

$$\min_{\{s^t\},\{p_{ra}^t\}} \quad \sum_{t=1}^{T} C^t(s^t) - \sum_{r=1}^{R} \sum_{a \in \mathcal{A}_r} U_{ra}(\mathbf{p}_{ra}) \tag{18a}$$

$$\text{subj. to } s^t = \sum_{r=1}^{R} \sum_{a \in \mathcal{A}_r} p_{ar}^t, \quad t = 1, \dots, T \tag{18b}$$

$$\mathbf{p}_{ra} \in \mathcal{P}_{ra}, a \in \mathcal{A}_r, \quad r = 1, \dots, R \tag{18c}$$

$$s^{\min} \le s^t \le s^{\max}, \quad t = 1, \dots, T. \tag{18d}$$

Clearly, the objective is optimizing the system's social welfare. The constraint in (18b) amounts to a balance equation for each period. Moreover, the set $\mathcal{P}_{ra}$ in (18c) represents the scheduling constraints for every appliance, while (18d) bounds the power provided by the LSE.

The problem in (18) is convex as long as $C^t(s^t)$ is convex, $U_{ra}(\mathbf{p}_{ra})$ is concave, and sets $\mathcal{P}_{ra}$ are convex. This is typically the case, and different works in the literature address DR using versions of the previous formulation [11], [56], [68], [23]. Various examples of appliance models—including batteries—together with their utility functions and constraint sets can also be found in the aforementioned works.

The problem in (18) as described so far amounts to energy consumption scheduling. Another instance of DR that can be described by the previous formulation is load curtailment. In this context, there is an energy deficit in the main grid for a particular time period, and the LSE must regulate the power consumption to cover for this deficit. The situation can be captured in (18) by setting $T = 1$ (single time period), and the power deficit as $s^{\min} = s^{\max} = s$. The cost C^t does not affect the optimization, while the negative of $U_{ra}(\mathbf{p}_{ra})$ represents the discomfort of the end-user due to the power curtailment, so the total discomfort $-\sum_{r,a} U_{ra}(\mathbf{p}_{ra})$ is minimized. This problem is addressed in [62], [39], and the references therein.

One of the main research objectives regarding (18) is to solve the scheduling problem in a distributed fashion, without having the functions $U_{ra}(\mathbf{p}_{ra})$ and sets $\mathcal{P}_{ra}$ communicated to the LSE to respect customer privacy. Algorithmic approaches typically entail message exchanges between the LSE and the users or among the users and lead to different pricing interpretations and models. Specific approaches include gradient projection [11]; block coordinate descent [56]; dual decomposition and subgradient method [23], [62]; the Vickrey-Clarke-Groves (VCG) mechanism [68]; Lagrangian relaxation and Newton method [62]; and dual decomposition with the bisection and Illinois methods [39].

Equation (18) refers to ahead-of-time scheduling. Real-time scheduling is also important. A real-time load response approach operating on a second-to-second scale is developed in [41] and references thereof. The aim is to have the aggregate power consumption of a set of thermostatically controlled loads (TCLs), such as A/C units, follow a desired signal. Model predictive control is employed to this end. Moreover, to come up with a simple description of the state space model pertaining to the set of TCLs, system identification ideas are brought to bear.

SINGLE-USER DR

The problems here focus on minimizing the total cost due to energy consumption or the peak instantaneous cost over a billing interval (or possibly a combination thereof). User comfort levels and preferences must also be taken into account.

Detailed modeling of appliance characteristics and scheduling capabilities typically introduces integer variables into the formulation, which is somewhat reminiscent of the unit commitment problem [cf. (17)]; see e.g., [64], [40], and [74], and the references therein. Solution approaches include standard mixed-integer programming

techniques—e.g., branch-and-bound, Lagrangian relaxation, dynamic programming—as well as random search methods such as genetic algorithms and particle swarm optimization. An interesting result is that when the problem is formulated over a continuous time horizon and accounts for the fact that appliances can be turned on or off anytime within the horizon, then it has zero duality gap [22].

Real-time approaches have also been pursued. A linear programming DR model with robustness against price uncertainty and time-series-based price prediction from period to period is developed in [15]. Moreover, [60] focuses on TCLs and, specifically, on a building with multiple zones, with each zone having its own heater. The aim is to minimize the peak instantaneous cost due to the power consumption of all heaters, while keeping each zone at a specified temperature interval. The problem is tackled through a decomposition into a master mixed-integer program and per zone heater control subproblems.

PLUG-IN (HYBRID) ELECTRIC VEHICLES

EVs (including PHEVs) are an important component of the future smart grid vision and are receiving a lot of attention. A global driving factor behind the research and development efforts on EVs is the environmental concern of the greenhouse gases emitted by the conventional fossil fuel-based transportation. As the future grids accommodate the renewable energy resources in an increasing scale, the carbon footprint is expected to be markedly curbed by high EV penetration. Electric driving also bears strategic relevance in the context of growing international tension over key natural resources including crude oil. From the simple perspective of improving overall energy efficiency, the electrification of transportation offers an excellent potential.

PEVs interact directly with the power grid through plug-in charging of built-in batteries. As such, judicious control and optimization of PEV charging pose paramount challenges and opportunities for the grid economy and efficiency. Since PEV charging constitutes an elastic energy load that can be time-shifted and warped, the benefits of DR are to be magnified when PEV charging is included in DR programs. In fact, as the scale of PEV adoption grows, it is clear that smart coordination of the charging task will become crucial to mitigate overloading of current distribution networks [13], [85], [18]. Without proper coordination, PEV charging can potentially create new peaks in the load curves with detrimental effects on generation cost. On the other hand, it is possible for the PEV aggregators that have control over a fleet of PEVs to provide ancillary services by modulating the charging rate in the vehicle-to-grid (V2G) concept [72]. This in turn allows the utilities to depend less on conventional generators with costly reserve capacities and facilitates mitigation of the volatility of renewable energy resources integrated to the grid [38]. The aforementioned topics are discussed in more detail next.

COORDINATION OF PEV CHARGING

It is widely recognized that uncoordinated PEV charging can pose serious issues on the economy of power generation and the quality of power delivered through the distribution networks. PEVs are equipped with batteries with sizable capacities, and it is not difficult to imagine that most people would opt to start charging their vehicles immediately after their evening commute, which is the time of the day that already exhibits a significant peak in power demand [18]. Fortunately, the smart grid AMI reviewed in the section "Demand Response" provides the groundwork for effective scheduling and control of PEV charging to meet the challenges and sustain mass adoption.

A variety of approaches have been proposed for PEV charging coordination. The power losses in the distribution network were minimized by optimizing the day-ahead charging rate schedules for given PEV charging demands in [13]. Real-time coordination was considered in [18], where the cost due to time-varying electricity price as well as the distribution losses were minimized by performing a simple sensitivity analysis of the cost and accommodating the charging priorities. Extending recent results on the globally optimal solution of the OPF problem via its Lagrangian dual [46], the optimality of similar approaches for PEV coordination problems was investigated in [71].

Interestingly, PEV charging can be also pursued in a distributed fashion. Further, optimizing feeder losses of distribution networks, load factor, and load variance are oftentimes equivalent problems [73]. Leveraging the latter, the minimization of load variance was investigated in [21]. Specifically, the optimal day-ahead charging profiles $\mathbf{r}_n := [r_n(1), \ldots, r_n(T)]$ for vehicle $n \in \{1, \ldots, N\}$ over a T-slot horizon, are obtained by solving

$$\min_{\mathbf{r}_1, \ldots, \mathbf{r}_N} \sum_{t=1}^{T} \left(D(t) + \sum_{n=1}^{N} r_n(t) \right)^2 \tag{19a}$$

$$\text{subj. to} \quad \underline{\mathbf{r}}_n \preceq \mathbf{r}_n \preceq \overline{\mathbf{r}}_n, \quad n = 1, \ldots, N \tag{19b}$$

$$\sum_{t=1}^{T} r_n(t) = B_n, \quad n = 1, \ldots, N, \tag{19c}$$

where $D(t)$ is the given base demand, $\underline{\mathbf{r}}_n$ and $\overline{\mathbf{r}}_n$ specify the limits on charging rates, and B_n represents the total energy expended for charging PEV n to the desired state-of-charge (SoC). The formulation is referred to as "valley-filling" in [21], as it schedules PEV loads in the valleys of the base load curve.

An optimal solution to (19) can be obtained iteratively [21]. Supposing that the initial pricing signal $p^k(t) = D(t)$, $t = 1, 2, \ldots, T$, and the initial charging profiles $r_n^k(t)$ are identically zero for iteration $k = 0$, each PEV n updates charging profiles $\mathbf{r}_n^{k+1}$ via

$$\min_{\mathbf{r}_n} \sum_{t=1}^{T} p^k(t) r_n(t) + \frac{N}{2} (r_n(t) - r_n^k(t))^2 \tag{20a}$$

$$\text{subj. to} \quad \underline{\mathbf{r}}_n \preceq \mathbf{r}_n \preceq \overline{\mathbf{r}}_n \ and \sum_{t=1}^{T} r_n(t) = B_n. \tag{20b}$$

A central entity such as the utility or a PEV aggregator then collects the profiles $\{\mathbf{r}_n^{k+1}\}$ from all PEVs, and updates the pricing signal as

$$p^{k+1}(t) = D(t) + \sum_{n=1}^{N} r_n^{k+1}(t). \tag{21}$$

The new pricing signals are then fed back to the PEVs and the procedure iterates until convergence. It is clear from (21) that the per-vehicle objective in (20a) corresponds to a first-order estimate of the overall objective in (19a), augmented with a proximal term. The overall procedure turns out to be a projected gradient search.

INTEGRATION WITH RENEWABLES AND V2G

It is only when the wide adoption of PEVs is coupled with the large-scale integration of renewable energy sources that the emission problem can be alleviated, as the conventional generation itself contributes heavily to the emission. However, renewable energy sources are by nature intermittent and often hard to predict accurately. By allowing the PEV batteries or fuel cells to supply their stored power to the grid based on the V2G concept, it was observed in [38] that photovoltaic (PV) resources harnessed by the EVs could competitively provide peak power (since the PV power becomes highest few hours earlier than the daily load peak quite predictably), and large-scale wind power could be stabilized for providing base power, via intelligent control. For specific control strategies to accomplish such benefits, formulations that maximize the profit for providing ancillary services were considered in [72] and references therein.

CHARGING DEMAND PREDICTION

An important prerequisite task to support the optimal coordination of PEVs is the modeling and prediction of the PEV charging demand. The probability distributions of the charging demand were characterized in [51] and references therein. Spatiotemporal PEV charging demand was analyzed for highway traffic scenarios using a fluid traffic model and a queuing model in [4]. However, there are many interesting issues remaining that deserve further research in this forecasting task.

RENEWABLES

The theme of the section "Economic Operation of Power Systems" has been economic scheduling of generators, which consume nonrenewable fuels. The subject of the present section is on including generation from renewable energy sources (RESs), with the two prime examples being wind and solar energy. RESs are random and intermittent, which makes them nondispatchable. That is, RESs are not only hard to predict but their intermittency gives rise to high variability even within time periods as short as ten minutes. Therefore, they cannot be readily treated as conventional generators and be included in the formulations of the section "Economic Operation of Power Systems." In this context, methods for integrating generation from RESs to the smart grid operations are outlined next.

FORECAST-BASED METHODS

To illustrate the forecast-based methods, recall the ED problem [cf. (13)] and suppose that there is also a wind power generator that can serve the load. The output of the wind power generator for the next time period is a random variable denoted by W. It is assumed that a forecast $\widehat{W}$ is available, and that the wind power generator has no cost (as it does not consume fuel). Then, the balance constraint is replaced by [cf. (13b)]

$$\sum_{i=1}^{N_g} P_{G_i} = P_L - \widehat{W} \tag{22}$$

while the remainder of the ED problem remains the same. Since the load is actually forecasted (cf. the section "Load and Electricity Price Forecasting"), the constraint in (22) essentially treats the uncertain RES no different than a negative load.

For the forecast to be accurate, the time period of ED is recommended to be short, such as 10 min. Building on this, a multiperiod ED is advocated in [32], where the main feature is a model-predictive control approach with a moving horizon. Specifically, the ED over multiple periods and accompanying forecasts is solved for e.g., six 10-min periods representing an hour. The generation is dispatched during the first period according to the obtained solution. Then, the horizon is moved, and a new multiperiod ED with updated forecasts is solved, whose results are applied only to the next period, and so on. Such a method can accommodate the ramping constraints, and is computationally efficient.

CHANCE-CONSTRAINED METHODS

To account for the random nature of RES in ED, the probability distribution of W comes handy. Specifically, the constraint is now that the supply-demand balance holds with high probability ε, say 99%. Hence, (22) is substituted by the chance constraint

$$\text{Prob}\left[\sum_{i=1}^{N_g} P_{G_i} + W \geq P_L\right] \geq \varepsilon. \tag{23}$$

Note that the equality of the balance equation has been replaced by an inequality in (23) because excess power from RESs can in principle be curtailed.

To solve the chance-constrained ED, the distribution of W must be known. For wind power, this is derived from the wind speed distribution and the speed-power output mapping of the generator [49]. The most typical speed distribution is Weibull, while the speed-power output mapping is nonlinear. Evidently, this approach poses formidable modeling and computing challenges when multiple RESs and their spatiotemporal correlation are considered. The probability that the load is not served [immediately obtained from the one in (23)] is often called loss of load probability. Related sophisticated methods that account for chance constraints are also described in [82]. An alternative approach not requiring the joint spatiotemporal wind distribution is presented in [92].

ROBUST (MINMAX) OPTIMIZATION

This approach postulates that the power generation from all RESs across space and time belongs to a deterministic uncertainty set. The aim is to minimize the worst-case operational costs, while setting the dispatchable generation and other optimization variables to such levels so that the balance is satisfied for any possible RES output within the uncertainty set. The main attractive feature here is that no detailed probabilistic models are needed. Only the uncertainty set must be obtained, e.g., from historical data or meteorological factors.

A robust version of UC [cf. (17)] is presented next. Following the notation of the section "Economic Operation of Power Systems," it is postulated that there are RESs with power output W_m^t per bus and time period. Let $\mathbf{w} := \{W_m^t\}_{m,t}$, and $\mathcal{W}$ denote the uncertainty set for $\mathbf{w}$. The optimization variables are set in two stages. The on/off variables $\mathbf{u} := \{u_m^t\}_{m,t}$ are chosen during the first stage. The power generation variables and bus angles are set after the RES power output is realized—which constitutes the second stage. Therefore, the power outputs and bus angles are functions of the commitments as well as the RES power outputs and are denoted as $P_{G_m}^t(\mathbf{u}, \mathbf{w})$ and $\theta_m^t(\mathbf{u}, \mathbf{w})$. The robust two-stage UC problem takes the form

$$\min_{\mathbf{u}, \{P_{G_m}^t(\mathbf{u},\mathbf{w}), \theta_m^t(\mathbf{u},\mathbf{w})\}} \sum_{t=1}^{T} \sum_{m=1}^{N_b} S_m^t(\{u_m^\tau\}_{\tau=0}^t)$$

$$+ \max_{\mathbf{w} \in \mathcal{W}} \sum_{t=1}^{T} \sum_{m=1}^{N_b} C_m^t(P_{G_m}^t(\mathbf{u},\mathbf{w})) \quad (24a)$$

subj. to $\qquad\qquad\qquad\qquad\qquad\qquad\qquad (24b)$

(17e), (17f), (17h)

$$\left.\begin{aligned} &(17c), (17d), (17g)\\ &P_{G_m}^t(\mathbf{u}, \mathbf{w}) + W_m^t = P_{L_m}^t \\ &\qquad\qquad + \sum_{n \in N_m}^{m} b_{mn}[\theta_m^t(\mathbf{u},\mathbf{w}) - \theta_n^t(\mathbf{u},\mathbf{w})] \end{aligned}\right\}$$

$$\forall \mathbf{w} \in \mathcal{W}. \quad (24c)$$

The objective (24a) consists of the startup/shutdown costs related to the on/off scheduling decisions, as well as the worst-case generation costs. The constraints in (24b) pertain only to the on/off variables and are identical to those in the UC problem. The remaining UC constraints must be satisfied for all possible realizations of the uncertain RES, as indicated in (24c).

The solution of problem (24) proceeds as follows. The on/off decisions u_m^t determine the UC ahead of the horizon $\{1, \ldots, T\}$. Then, at each period, after the RES power output is realized, functions $P_{G_m}^t(\mathbf{u}, \mathbf{w})$ yield the power generation dispatch. The punch line of this two-stage robust program is that generation becomes adaptive to the RES uncertainty. Solution methods typically involve pertinent decompositions and approximations [93], [6].

A different robust approach for energy management in microgrids is pursued in [91]. Microgrids are power systems comprising many distributed energy resources (DERs) and electricity end users, all deployed across a limited geographical area.

Depending on their origin, DERs can come either from distributed generation (DG), meaning small-scale power generators based on fuels or RESs, or from distributed storage (DS), such as batteries (see Figure 9). The case where a microgrid is connected to the main grid, while energy can be sold to or purchased from the main grid, is considered in [91]. The approach adopts a worst-case transaction cost. Leveraging the dual decomposition, its solution is obtained in a distributed fashion by local controllers of the DG units and dispatchable loads.

SCENARIO-BASED STOCHASTIC PROGRAMMING
This method also amounts to a two-stage adaptive approach, albeit in a different manner than the previous one. Here, a discrete set of possible scenarios for the RES power output across the horizon is considered. For instance, considering 8 h with power output taking seven possible values, there are 7^8 possible scenarios. A probability is attached to a each of these scenarios (or only to a selection thereof). Similar to (24a), the objective includes startup/shutdown costs due to on/off scheduling. But instead of a worst-case part, the expected cost of generation dispatch with respect to the scenario probabilities is included in the objective.

The aforementioned approach is pursued in [9], whereby the scheduling of spinning reserves is also included. Spinning reserve is generation capacity that is not currently used to serve the load but is connected to the system (spinning) and is available to serve the load in case there is loss of generation. Spinning reserves are instrumental components of any power system, and the premise here is that they can be provisioned in a manner adaptive to the RES uncertainty.

MULTISTAGE STOCHASTIC DYNAMIC PROGRAMMING
The aim here is to address the decision-making challenges for an LSE obtaining energy from the market as well as from RESs (cf. Figure 8). The LSE may procure energy in the day-ahead market, as well as in the real-time market, which is a decision made on-the-fly during the scheduling horizon. The energy from RESs is typically cost free, but random. In addition, the LSE must provide power to the end users during the horizon, and take the associated pricing decisions. The multiple-timescale feature reflects exactly the resolution over day-ahead, hour-ahead, and real time (e.g., at the scale of minutes) decisions. Multistage dynamic programming captures the coupling of decisions across time due to end users' power requirements—e.g., total energy
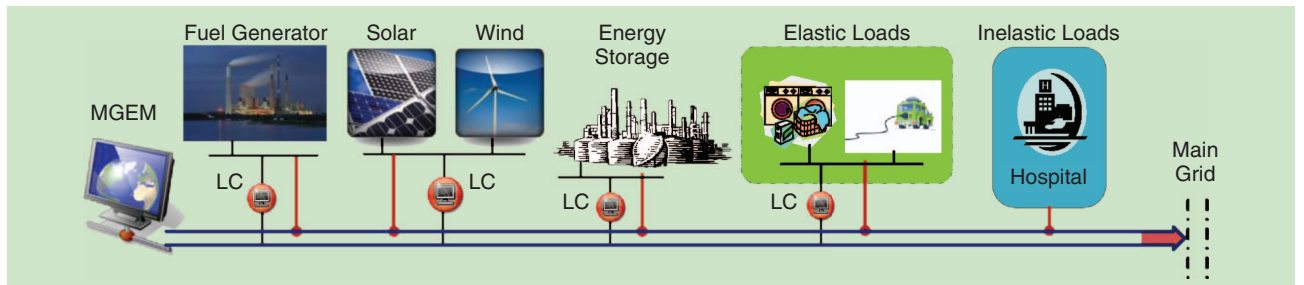
[FIG9] Distributed control and computation architecture of a microgrid system. The microgrid energy manager (MGEM) coordinates the local controllers (LCs) of DERs and dispatchable loads.

requested over a specified interval or price-adaptive random opportunistic demand [33], [30].

NETWORK OPTIMIZATION BASED ON LONG-TERM AVERAGE CRITERIA

This approach relies on queueing-theoretic and Lyapunov-based stochastic network optimization methods popular in resource allocation tasks for wireless networks. A load-serving entity obtaining energy from the market as well as from RESs is considered in [59], [31]. The objective is cost minimization or social welfare maximization in a long-term average fashion over an infinite horizon, and the decision variables include pricing and power provided to end users; see [43] for energy storage management policies.

OPEN ISSUES

Although the SP research efforts on the power grid are fast growing, there are many open issues awaiting investigation. Regarding situational awareness, integrating local power grids into interconnections poses modeling and computational challenges. Monitoring grids of dimensionality and detail calls for scalable and modular algorithms. To communicate and process the massive volume of measurements in real time with tractable complexity, the issues related to compressing, layering, relaying, and storing these data must be considered too. The "big data" challenges further extend to addressing the missing data and the under-determinacy of the resultant systems of equations, as well as model reduction tasks, for which contemporary statistical learning approaches could provide viable solutions.

The control and optimization dimensions entail conventional generation as well as RESs, interconnected via transmission and distribution networks, serving large industrial customers and residential end users with smart appliances and PHEVs, as well as microgrids with distributed generation and storage. SP researchers can cross-fertilize their ample expertise on resource allocation gained in the context of communication networks to optimize power network operations. Major challenges include the successful coordination of system-level economic operations such as OPF and UC, while embracing small-scale end users through DR and coordinated PHEV charging. Integrating random and intermittent RESs across all levels poses further challenges. Issues related to leveraging the markedly improved monitoring modalities in grid operations are worth careful study. Although research efforts tackling individual problems have yielded promising outcomes, achieving the grand goal of reliable and efficient grid operations still calls for novel formulations, insightful approximations, integration, and major algorithmic breakthroughs.

AUTHORS

Georgios B. Giannakis (georgios@umn.edu) received his Ph.D. degree from the University of Southern California in 1986. Since 1999, he has been with the University of Minnesota, where he holds the ADC chair in wireless telecommunications in the Department of Electrical and Computer Engineering, and where he serves as director of the Digital Technology Center. His interests are in the areas of communications, networking, and statistical signal processing—subjects on which he has published more than 350 journal and 580 conference papers, 20 book chapters, two edited books, and two research monographs (h-index 104). His current research focuses on sparsity and big data analytics, cognitive networks, renewables, the power grid, and social networks. He is the (co)inventor of 21 patents and the (co)recipient of eight best paper awards from the IEEE Communications and Signal Processing Societies. He is a Fellow of the IEEE and EURASIP, and has also received technical achievement awards from the IEEE Signal Processing Society and EURASIP.

Vassilis Kekatos (kekatos@umn.edu) received his diploma, M.S. degree, and Ph.D. degree in computer engineering and informatics from the University of Patras, Greece, in 2001, 2003, and 2007, respectively. He is currently a postdoctoral associate with the Department of Electrical and Computer Engineering at the University of Minnesota. In 2009, he received a Marie Curie fellowship. In 2012, he worked as a consultant for Windlogics Inc. His research interests lie in the area of statistical signal processing with emphasis on power grid applications, compressive sampling, and wireless communications. He is a Member of the IEEE.

Nikolaos Gatsis (gatsisn@umn.edu) received the diploma degree in electrical and computer engineering from the University of Patras, Greece, in 2005 with honors. He completed his graduate studies at the University of Minnesota, where he received the M.S. degree in electrical engineering in 2010 and the Ph.D. degree in electrical engineering (with a minor in mathematics) in 2012. He was a research intern at Mitsubishi Electric Research Laboratories, Boston, Massachusetts, in 2011. He is currently a postdoctoral associate with the Department of Electrical and Computer Engineering at the University of Minnesota, Minneapolis. He will be joining the Department of Electrical and Computer Engineering at the University of Texas at San Antonio as an assistant professor in the fall. His research interests are in the areas of smart power grids, renewable energy management, wireless communications, and networking, with an emphasis on optimization methods and resource management. He is a Member of the IEEE.

Seung-Jun Kim (seungjun@umn.edu) received his B.S. and M.S. degrees from Seoul National University, Korea, in 1996 and 1998, respectively, and his Ph.D. degree from the University of California at Santa Barbara in 2005, all in electrical engineering. From 2005 to 2008, he worked for NEC Laboratories America in Princeton, New Jersey, as a research staff member. Currently, he is with the Department of Electrical and Computer Engineering at the University of Minnesota, where he is a research assistant professor. His research interests span signal processing, optimization and learning techniques with applications to wireless communication and networking, smart power grids, and biological and social networks. He is a Senior Member of the IEEE.

Hao Zhu (zhuh@umn.edu) received her bachelor's degree from Tsinghua University, China, in 2006 and the M.S. and Ph.D. degrees from the University of Minnesota, Twin Cities, in 2009 and 2012, all in electrical engineering. She is currently a postdoctoral research associate with the Power and Energy Systems Group at the University of Illinois, Urbana-Champaign, where she will start as an assistant professor in the spring of 2014. Her current research interests include power system monitoring and dynamics, distribution system operations and control, and the smart grid. She is a Member of the IEEE.

Bruce F. Wollenberg (wollenbe@umn.edu) received the B.S.E.E. degree and the M.Eng. degree in electric power engineering from Rensselaer Polytechnic Institute, Troy, New York, in 1964 and 1966, respectively, and the Ph.D. degree in systems engineering from the University of Pennsylvania, Philadelphia, in 1974. He became a professor of electrical engineering in the Department of Electrical and Computer Engineering at the University of Minnesota, Minneapolis, in September 1989. He is a member of the National Academy of Engineering and currently directs the University of Minnesota Center for Electric Energy. His main research interests are the application of mathematical analysis to power system operation and planning problems. He is a Life Fellow of the IEEE.

REFERENCES

[1] A. Abur and A. Gómez-Expósito, *Power System State Estimation: Theory and Implementation*. New York: Marcel Dekker, 2004.

[2] S. M. Amin and B. F. Wollenberg, "Toward a smart grid: Power delivery for the 21st century," *IEEE Power Energy Mag.*, vol. 3, no. 5, pp. 34–41, 2005.

[3] N. Amjady and M. Hemmati, "Energy price forecasting: Problems and proposals for such predictions," *IEEE Power Energy Mag.*, vol. 4, no. 2, pp. 20–29, Mar.–Apr. 2006.

[4] S. Bae and A. Kwasinski, "Spatial and temporal model of electric vehicle charging demand," *IEEE Trans. Smart Grid*, vol. 3, no. 1, pp. 394–403, Mar. 2012.

[5] D. P. Bertsekas, G. S. Lauer, N. R. Sandell Jr., and T. A. Posbergh, "Optimal short-term scheduling of large-scale power systems," *IEEE Trans. Autom. Contr.*, vol. 28, no. 1, pp. 1–11, Jan. 1983.

[6] D. Bertsimas, E. Litvinov, X. Sun, J. Zhao, and T. Zheng, "Adaptive robust optimization for the security constrained unit commitment problem," *IEEE Trans. Power Syst.,* vol. 28, no. 1, pp. 52–63, Feb. 2013.

[7] E. A. Blood, B. H. Krogh, and M. D. Ilić, "Electric power system static state estimation through Kalman filtering and load forecasting," in *Proc. IEEE Power Energy Society General Meeting*, Pittsburgh, PA, 2008, pp. 1–6.

[8] S. Blumsack, P. Hines, M. Patel, C. Barrows, and E. Cotilla Sanchez, "Defining power network zones from measures of electrical distance," in *Proc. IEEE Power Energy Society General Meeting*, Calgary, AB, Canada, July 2009, pp. 1–8.

[9] F. Bouffard and F. D. Galiana, "Stochastic security for operations planning with significant wind power generation," *IEEE Trans. Power Syst.*, vol. 23, no. 2, pp. 306–316, May 2008.

[10] M. C. Caramanis, R. E. Bohn, and F. C. Schweppe, "Optimal spot pricing: Theory and practice," *IEEE Trans. Power App. Syst. (1963–1985)*, vol. 101, no. 9, pp. 3234–3245, Sept. 1982.

[11] L. Chen, N. Li, L. Jiang, and S. H. Low, "Optimal demand response: Problem formulation and deterministic case," in *Control and Optimization Methods for Electric Smart Grids*, A. Chakrabortty and M. D. Ilić, Eds. New York: Springer-Verlag, 2012, pp. 63–85.

[12] R. D. Christie, B. F. Wollenberg, and I. Wangensteen, "Transmission management in the deregulated environment," *Proc. IEEE*, vol. 88, no. 2, pp. 170–195, Feb. 2000.

[13] K. Clement-Nys, E. Haesen, and J. Driesen, "The impact of charging plug-in hybrid electric vehicles on a residential distribution grid," *IEEE Trans. Power Syst.*, vol. 25, no. 1, pp. 2010–2019, Feb. 2010.

[14] K. A. Clements, G. R. Krumpholz, and P. W. Davis, "Power system state estimation with measurement deficiency: An observability/measurement placement algorithm," *IEEE Trans. Power App. Syst. (1963–1985)*, vol. 102, no. 7, pp. 2012–2020, July 1983.

[15] A. J. Conejo, J. M. Morales, and L. Baringo, "Real-time demand response model," *IEEE Trans. Smart Grid*, vol. 1, no. 3, pp. 236–242, Dec. 2010.

[16] A. J. Conejo, S. de la Torre, and M. Canas, "An optimization approach to multiarea state estimation," *IEEE Trans. Power Syst.*, vol. 22, no. 1, pp. 213–221, Feb. 2007.

[17] E. Dall'Anese, G. B. Giannakis, and B. F. Wollenberg, "Optimization of unbalanced power distribution networks via semidefinite relaxation," in *Proc. North American Power Symp.*, Urbana-Champaign, IL, Sept. 2012, pp. 1–6.

[18] S. Deilami, A. S. Masoum, P. S. Moses, and M. A. S. Masoum, "Real-time coordination of plug-in electric vehicle charging in smart grids to minimize power losses and improve voltage profile," *IEEE Trans. Smart Grid*, vol. 2, no. 3, pp. 456–467, Sept. 2011.

[19] R. Ebrahimian and R. Baldick, "State estimation distributed processing," *IEEE Trans. Power Syst.*, vol. 15, no. 4, pp. 1240–1246, Nov. 2000.

[20] R. Emami and A. Abur, "Tracking changes in the external network model," in *Proc. North American Power Symp.*, Arlington, TX, Sept. 2010, pp. 1–6.

[21] L. Gan, U. Topcu, and S. Low, "Optimal decentralized protocol for electric vehicle charging," in *Proc. 50th IEEE Conf. Decision and Control*, Orlando, FL, Dec. 2011, pp. 5798–5804.

[22] N. Gatsis and G. B. Giannakis, "Residential demand response with interruptible tasks: Duality and algorithms," in *Proc. 50th IEEE Conf. Decision and Control*, Orlando, FL, Dec. 2011, pp. 1–6.

[23] N. Gatsis and G. B. Giannakis, "Residential load control: Distributed scheduling and convergence with lost AMI messages," *IEEE Trans. Smart Grid*, vol. 3, no. 2, pp. 770–786, June 2012.

[24] A. M. Giacomoni, S. M. Amin, and B. F. Wollenberg, "Reconfigurable interdependent infrastructure systems: Advances in distributed sensing, modeling, and control," in *Proc. American Control Conf.*, San Francisco, CA, June–July 2011, pp. 4160–4165.

[25] A. Gómez-Expósito, A. J. Conejo, and C. Canizares, Eds., *Electric Energy Systems, Analysis and Operation*. Boca Raton, FL: CRC Press, 2009.

[26] A. Gómez-Expósito and A. de la Villa Jaén, "Reduced substation models for generalized state estimation," *IEEE Trans. Power Syst.*, vol. 16, no. 4, pp. 839–846, Nov. 2001.

[27] A. Gómez-Expósito, A. Abur, A. de la Villa Jaén, and C. Gómez-Quiles, "A multilevel state estimation paradigm for smart grids," *Proc. IEEE*, vol. 99, no. 6, pp. 952–976, June 2011.

[28] A. Gómez-Expósito, A. de la Villa Jaén, C. Gómez-Quiles, P. Rousseaux, and T. V. Cutsem, "A taxonomy of multi-area state estimation methods," *Electric Power Syst. Res.*, vol. 81, no. 4, pp. 1060–1069, 2011.

[29] K. Hamilton and N. Gulhar, "Taking demand response to the next level," *IEEE Power Energy Mag.*, vol. 8, no. 3, pp. 60–65, May–June 2010.

[30] M. He, S. Murugesan, and J. Zhang, "Multiple timescale dispatch and scheduling for stochastic reliability in smart grids with wind generation integration," in *Proc. IEEE INFOCOM*, Shanghai, China, Apr. 2011, pp. 461–465.

[31] L. Huang, J. Walrand, and K. Ramchandran, "Optimal power procurement and demand response with quality-of-usage guarantees," in *Proc. IEEE Power Energy Society General Meeting*, San Diego, CA, 2012, pp. 1–8.

[32] M. D. Ilić, L. Xie, and J.-Y. Joo, "Efficient coordination of wind power and price-responsive demand. Part I: Theoretical foundations," *IEEE Trans. Power Syst.*, vol. 26, no. 4, pp. 1875–1884, Nov. 2011.

[33] L. Jiang and S. H. Low, "Real-time demand response with uncertain renewable energy in smart grid," in *Proc. 49th Allerton Conf. Communications, Control, and Computing*, Monticello, IL, Sept. 2011, pp. 1334–1341.

[34] V. Kekatos and G. B. Giannakis, "Distributed robust power system state estimation," *IEEE Trans. Power Syst.,* vol. 28, no. 2, pp. 1617–1626, May 2013.

[35] V. Kekatos, G. B. Giannakis, and B. F. Wollenberg, "Optimal placement of phasor measurement units via convex relaxation," *IEEE Trans. Power Syst.*, vol. 27, no. 3, pp. 1521–1530, Aug. 2012.

[36] V. Kekatos, M. Light, S. Veeramachaneni, and G. B. Giannakis, "Day-ahead electricity market forecasting," in *Proc. IEEE PES Innovative Smart Grid Technologies*, Washington, DC, Feb. 2013, pp. 1–5.

[37] V. Kekatos and G. B. Giannakis, "Joint power system state estimation and breaker status identification," in *Proc. North American Power Symp.*, Urbana-Champaign, IL, Sept. 2012, pp. 1–6.

[38] W. Kempton and J. Tomić, "Vehicle-to-grid power implementation: From stabilizing the grid to supporting large-scale renewable energy," *J. Power Sources*, vol. 144, no. 1, pp. 280–294, June 2005.

[39] H. Kim, Y.-J. Kim, K. Yang, and M. Thottan, "Cloud-based demand response for smart grid: Architecture and distributed algorithms," in *Proc. 2nd Int. Conf. Smart Grid Communications*, Brussels, Belgium, Oct. 2011, pp. 416–421.

[40] S.-J. Kim and G. B. Giannakis, "Scalable and robust demand response with mixed-integer constraints," *IEEE Trans. Smart Grid*. [Online]. Available: http://dx.doi.org/10.1109/TSG.2013.2257893

[41] S. Koch, J. L. Mathieu, and D. S. Callaway, "Modeling and control of aggregated heterogeneous thermostatically controlled loads for ancillary services," in *Proc. Power Systems Computation Conf.*, Stockholm, Sweden, Aug. 2011, pp. 1–7.

[42] O. Kosut, L. Jia, J. Thomas, and L. Tong, "Malicious data attacks on the smart grid," *IEEE Trans. Smart Grid*, vol. 2, no. 4, pp. 645–658, Dec. 2011.

[43] I. Koutsopoulos, V. Hatzi, and L. Tassiulas, "Optimal energy and storage control policies for the smart power grid," in *Proc. 2nd IEEE Int. Conf. Smart Grid Communications*, Brussels, Belgium, Oct. 2011, pp. 475–480.

[44] P. Kundur, *Power System Stability and Control*. New York: McGraw-Hill, 1994.

[45] A. Y. S. Lam, B. Zhang, A. Dominguez-Garcia, and D. Tse, "Optimal distributed voltage regulation in power distribution networks," submitted for publication.

[46] J. Lavaei and S. H. Low, "Zero duality gap in optimal power flow problem," *IEEE Trans. Power Syst.*, vol. 27, no. 1, pp. 92–107, Feb. 2012.

[47] J. Li, C.-C. Liu, and K. Schneider, "Controlled partitioning of a power network considering real and reactive power balance," *IEEE Trans. Smart Grid*, vol. 1, no. 3, pp. 261–269, Dec. 2010.

[48] Q. Li, R. Negi, and M. D. Ilić, "Phasor measurement units placement for power system state estimation: A greedy approach," in *Proc. IEEE PES General Meeting*, Detroit, July 2011, pp. 1–8.

[49] X. Liu, "Economic load dispatch constrained by wind power availability: A wait-and-see approach," *IEEE Trans. Smart Grid*, vol. 1, no. 3, pp. 347–355, Dec. 2010.

[50] Y. Liu, P. Ning, and M. K. Reiter, "False data injection attacks against state estimation in electric power grids," *ACM Trans. Inform. Syst. Security*, vol. 14, no. 1, pp. 13:1–13:33, May 2011.

[51] A. Lojowska, D. Kurowicka, G. Papaefthymiou, and L. van der Sluis, "Stochastic modeling of power demand due to EVs using copula," *IEEE Trans. Power Syst.*, vol. 27, no. 4, pp. 1960–1968, Nov. 2012.

[52] Z.-Q. Luo, W. K. Ma, A. M. C. So, Y. Ye, and S. Zhang, "Semidefinite relaxation of quadratic optimization problems," *IEEE Signal Processing Mag.*, vol. 27, no. 3, pp. 20–34, 2010.

[53] N. M. Manousakis, G. N. Korres, and P. S. Georgilakis, "Taxonomy of PMU placement methodologies," *IEEE Trans. Power Syst.*, vol. 27, no. 2, pp. 1070–1077, May 2012.

[54] G. Mateos and G. B. Giannakis, "Load curve data cleansing and imputation via sparsity and low rank," in *Proc. 3rd Int. Conf. Smart Grid Communications*, Tainan, Taiwan, Nov. 2012, pp. 653–658.

[55] F. Milano, "An open source power system analysis toolbox," *IEEE Trans. Power Syst.*, vol. 20, no. 3, pp. 1199–1206, Aug. 2005.

[56] A.-H. Mohsenian-Rad, V. S. W. Wong, J. Jatskevich, R. Schober, and A. Leon-Garcia, "Autonomous demand side management based on game-theoretic energy consumption scheduling for the future smart grid," *IEEE Trans. Smart Grid*, vol. 1, no. 3, pp. 320–331, Dec. 2010.

[57] A. Monticelli, "Electric power system state estimation," *Proc. IEEE*, vol. 88, no. 2, pp. 262–282, Feb. 2000.

[58] A. Monticelli and F. F. Wu, "Network observability: Theory," *IEEE Trans. Power App. Syst. (1963–1985)*, vol. 104, no. 5, pp. 1042–1048, May 1985.

[59] M. J. Neely, A. S. Tehrani, and A. G. Dimakis, "Efficient algorithms for renewable energy allocation to delay tolerant consumers," in *Proc. 1st Int. Conf. Smart Grid Communications*, Gaithersburg, MD, Oct. 2010, pp. 549–554.

[60] T. X. Nghiem, M. Behl, R. Mangharam, and G. J. Pappas, "Green scheduling of control systems for peak demand reduction," in *Proc. 50th IEEE Conf. Decision and Control*, Orlando, FL, Dec. 2011, pp. 5131–5136.

[61] R. F. Nuqui and A. G. Phadke, "Phasor measurement unit placement techniques for complete and incomplete observability," *IEEE Trans. Power Delivery*, vol. 20, no. 4, pp. 2381–2388, Oct. 2005.

[62] A. Papavasiliou, H. Hindi, and D. Greene, "Market-based control mechanisms for electric power demand response," in *Proc. 49th IEEE Int. Conf. Decision and Control*, Dec. 2010, pp. 1891–1898.

[63] F. Pasqualetti, F. Dorfler, and F. Bullo, "Attack detection and identification in cyber-physical systems," *IEEE Trans. Autom. Contr.* [Online]. Available: http://dx.doi.org/10.1109/TAC.2013.2266831

[64] M. A. A. Pedrasa, T. D. Spooner, and I. F. MacGill, "Coordinated scheduling of residential distributed energy resources to optimize smart home energy services," *IEEE Trans. Smart Grid*, vol. 1, no. 2, pp. 134–143, Sept. 2010.

[65] A. G. Phadke and J. S. Thorp, *Synchronized Phasor Measurements and Their Applications*. New York: Springer-Verlag, 2008.

[66] A. G. Phadke, J. S. Thorp, and K. J. Karimi, "State estimation with phasor measurements," *IEEE Trans. Power Syst.*, vol. 1, no. 1, pp. 233–238, Feb. 1986.

[67] P. Rousseaux, T. Van Cutsem, and T. E. Dy Liacco, "Whither dynamic state estimation?" *Int. J. Electr. Power Energy Syst.*, vol. 12, no. 2, pp. 104–116, 1990.

[68] P. Samadi, R. Schober, and V. W. S. Wong, "Optimal energy consumption scheduling using mechanism design for the future grid," in *Proc. 2nd IEEE Int. Conf. Smart Grid Communications*, Brussels, Belgium, Oct. 2011, pp. 369–374.

[69] F. C. Schweppe, J. Wildes, and D. Rom, "Power system static state estimation: Parts I, II, and III," *IEEE Trans. Power App. Syst. (1963–1985)*, vol. 89, pp. 120–135, Jan. 1970.

[70] M. Shahidehpour, H. Yamin, and Z. Li, *Market Operations in Electric Power Systems: Forecasting, Scheduling, and Risk Management*. New York: IEEE-Wiley Interscience, 2002.

[71] S. Sojoudi and S. H. Low, "Optimal charging of plug-in hybrid electric vehicles in smart grids," in *Proc. IEEE Power and Energy Society General Meeting*, Detroit, MI, July 2011, pp. 1–6.

[72] E. Sortomme and M. A. El-Sharkawi, "Optimal scheduling of vehicle-to-grid energy and ancillary services," *IEEE Trans. Smart Grid*, vol. 3, no. 1, pp. 351–359, Mar. 2012.

[73] E. Sortomme, M. M. Hindi, S. D. J. MacPherson, and S. S. Venkata, "Coordinated charging of plug-in hybrid electric vehicles to minimize distribution system losses," *IEEE Trans. Smart Grid*, vol. 2, no. 1, pp. 198–205, Mar. 2011.

[74] K. C. Sou, J. Weiner, H. Sandberg, and K. H. Johansson, "Scheduling smart home appliances using mixed integer linear programming," in *Proc. 50th IEEE Conf. Decision and Control*, Orlando, FL, Dec. 2011, pp. 5144–5149.

[75] S. Takriti and J. R. Birge, "Using integer programming to refine Lagrangian-based unit commitment solutions," *IEEE Trans. Power Syst.*, vol. 15, no. 1, pp. 151–156, Feb. 2000.

[76] J. E. Tate and T. J. Overbye, "Line outage detection using phasor angle measurements," *IEEE Trans. Power Syst.*, vol. 23, no. 4, pp. 1644–1652, Nov. 2008.

[77] J. E. Tate and T. J. Overbye, "Double line outage detection using phasor angle measurements," in *Proc. IEEE Power and Energy Society General Meeting*, Calgary, AB, Canada, July 2009, pp. 1–5.

[78] V. Terzija, G. Valverde, D. Cai, P. Regulski, V. Madani, J. Fitch, S. Skok, M. M. Begovic, and A. Phadke, "Wide-area monitoring, protection, and control of future electric power networks," *Proc. IEEE*, vol. 99, no. 1, pp. 80–93, Jan. 2011.

[79] D. Trudnowski and J. Pierre, "Signal processing methods for estimating small-signal dynamic properties from measured responses," in *Inter-Area Oscillations in Power Systems* (Power Electronics and Power Systems series), A. R. Messina, Ed. New York: Springer-Verlag, 2009, pp. 1–36.

[80] University of Washington. Power systems test case archive [Online]. Available: http://www.ee.washington.edu/research/pstca/

[81] G. Valverde and V. Terzija, "Unscented Kalman filter for power system dynamic state estimation," *IET Generation, Transmission, Distribution*, vol. 5, no. 1, pp. 29–37, 2011.

[82] P. P. Varaiya, F. F. Wu, and J. W. Bialek, "Smart operation of smart grid: Risk-limiting dispatch," *Proc. IEEE*, vol. 99, no. 1, pp. 40–57, Jan. 2011.

[83] D. J. Watts and S. H. Strogatz, "Collective dynamics of 'small-world' networks," *Nature*, vol. 393, pp. 440–442, June 1998.

[84] A. J. Wood and B. F. Wollenberg, *Power Generation, Operation, and Control*, 2nd ed. New York: Wiley, 1996.

[85] D. Wu, D. C. Aliprantis, and K. Gkritza, "Electric energy and power consumption by light-duty plug-in electric vehicles," *IEEE Trans. Power Syst.*, vol. 26, no. 2, pp. 738–746, May 2011.

[86] L. Wu and M. Shahidehpour, "A hybrid model for day-ahead price forecasting," *IEEE Trans. Power Syst.*, vol. 25, no. 3, pp. 1519–1530, Aug. 2010.

[87] W. A. Wulf. (2010). Great achievements and grand challenges. *The Bridge* [Online]. *30(3–4)*, pp. 5–10 . Available: http://www.greatachievements.org/

[88] L. Xie, D.-H. Choi, and S. Kar, "Cooperative distributed state estimation: Local observability relaxed," in *Proc. IEEE PES General Meeting*, Detroit, MI, July 2011.

[89] L. Xie, Y. Mo, and B. Sinopoli, "Integrity data attacks in power market operations," *IEEE Trans. Smart Grid*, vol. 2, no. 4, pp. 659–666, Dec. 2011.

[90] W. Xu, M. Wang, and A. Tang, "On state estimation with bad data detection," in *Proc. IEEE Conf. Decision and Control and European Control Conf. (CDC-ECC)*, Orlando, FL, Dec. 2011, pp. 5989–5994.

[91] Y. Zhang, N. Gatsis, and G. B. Giannakis, "Robust energy management for microgrids with high-penetration renewables," *IEEE Trans. Sustainable Energy*. [Online]. Available: http://dx.doi.org/10.1109/TSTE.2013.2255135

[92] Y. Zhang, N. Gatsis, and G. B. Giannakis, "Risk-constrained energy management with multiple wind farms," in *Proc. IEEE PES Innovative Smart Grid Technologies*, Washington, DC, Feb. 2013, pp. 510–515.

[93] L. Zhao and B. Zeng, "Robust unit commitment problem with demand response and wind energy," in *Proc. Power and Energy Society General Meeting*, San Diego, CA, July 2012, pp. 1–8.

[94] N. Zhou, D. J. Trudnowski, J. W. Pierre, and W. Mittelstadt, "Electromechanical mode online estimation using regularized robust RLS methods," *IEEE Trans. Power Syst.*, vol. 23, no. 4, pp. 1670–1680, Nov. 2008.

[95] H. Zhu and G. B. Giannakis, "Estimating the state of AC power systems using semidefinite programming," in *Proc. 43rd North American Power Symp.*, Boston, MA, Aug. 2011, pp. 1–7.

[96] H. Zhu and G. B. Giannakis, "Multi-area state estimation using distributed SDP for nonlinear power systems," in *Proc. 3rd Int. Conf. Smart Grid Communications*, Tainan, Taiwan, Nov. 2012, pp. 623–628.

[97] H. Zhu and G. B. Giannakis, "Robust power system state estimation for the nonlinear AC flow model," in *Proc. North American Power Symp.*, Urbana-Champaign, IL, Sept. 2012, pp. 1–6.

[98] H. Zhu and G. B. Giannakis, "Sparse overcomplete representations for efficient identification of power line outages," *IEEE Trans. Power Syst.*, vol. 27, no. 4, pp. 2215–2224, Nov. 2012.

[99] R. D. Zimmerman, C. E. Murillo-Sanchez, and R. J. Thomas, "MATPOWER: Steady-state operations, planning and analysis tools for power systems research and education," *IEEE Trans. Power Syst.*, vol. 26, no. 1, pp. 12–19, Feb. 2011. **SP**